Journal Pre-proofs

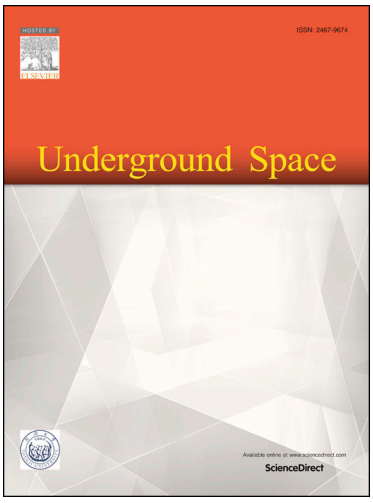

Rockburst in underground excavations: A review of mechanism, classification, and prediction methods

Mahdi Askaripour, Ali Saeidi, Alain Rouleau, Patrick Mercier-Langevin

PII: S2467-9674(22)00002-2
DOI: https://doi.org/10.1016/j.undsp.2021.11.008
Reference: UNDSP 221

To appear in: *Underground Space*

Received Date: 6 August 2020
Revised Date: 2 November 2021
Accepted Date: 11 November 2021

Please cite this article as: M. Askaripour, A. Saeidi, A. Rouleau, P. Mercier-Langevin, Rockburst in underground excavations: A review of mechanism, classification, and prediction methods, *Underground Space* (2022), doi: https://doi.org/10.1016/j.undsp.2021.11.008

Rockburst in underground excavations: A review of mechanism, classification, and prediction methods

Mahdi Askaripour [1,*] , Ali Saeidi [1], Alain Rouleau [1], Patrick Mercier-Langevin [2]

[1] Department of Applied Sciences, University of Quebec at Chicoutimi, Chicoutimi G7H 2B1, Canada

[2] Geological Survey of Canada, Quebec City, QC G1K 9A9, Canada

* Corresponding author: Department of Applied Sciences, Université du Québec à Chicoutimi, Chicoutimi (Québec) G7H 2B1, Canada. Email: mahdi.askaripour1@uqac.ca

Abstract

Technical challenges have always been part of underground mining activities, however, some of these challenges grow in complexity as mining occurs in deeper and deeper settings. One such challenge is rock mass stability and the risk of rockburst events. To overcome these challenges, and to limit the risks and impacts of events such as rockbursts, advanced solutions must be developed and best practices implemented. Rockbursts are common in underground mines and substantially threaten the safety of personnel and equipment, and can cause major disruptions in mine development and operations. Rockbursts consist of violent wall rock failures associated with high energy rock projections in response to the instantaneous stress release in rock mass under high strain conditions. Therefore, it is necessary to develop a good understanding of the conditions and mechanisms leading to a rockburst, and to improve risk assessment methods. The capacity to properly estimate the risks of rockburst occurrence is essential in underground operations. However, a limited number of studies have examined and compared yet different empirical methods of rockburst. The current understanding of this important hazard in the mining industry is summarized in this paper to provide the necessary perspective or tools to best assess the risks of rockburst occurrence in deep mines. The various classifications of rockbursts and their mechanisms are discussed. The paper also reviews the current empirical methods of rockburst prediction, which are mostly dependent on geomechanical parameters of the rock such as uniaxial compressive strength of the rock, as well as its tensile strength and elasticity modulus. At the end of this paper, some current achievements and limitations of empirical methods are discussed.

Keywords: Rockburst; Empirical methods; Underground instability; Rockburst prediction methods

1 Introduction

With a growing demand for mineral resources, the optimization of mining and metals recovery techniques, and the gradual depletion of near surface resources, the industry is mining at increasingly greater depths below surface (Lippmann-Pipke et al., 2011). Underground operations

at 2000 m below surface or more are becoming more and more common, with a few examples at more than 4000 m. One of the most important challenges that underground mining operations must face is the instability of the rock mass (Aydan & Genis, 2001). The shape and type of rock mass instability in deep excavations depend on several factors, including inherent properties of rock, such as strength and brittleness, and external conditions, such as magnitude of in situ stresses, dynamic disturbance, excavation sequence and geological structure (Meng et al., 2017). However, the magnitude of in situ stresses and the quality of rock mass play a significant role in the determination of the rock mass instability in underground excavations. Based on these parameters, nine types of rock mass instability were defined by Hoek and Brown (1980) (Fig. 1). The geological strength index (GSI) and a stress parameter (ratio of the maximum principal stress to the uniaxial compressive strength of the rock) are considered in this classification. In low-stress environments, the distribution and the continuity of natural fractures control the failure process in the rock; whereas, in high-stress environments, the failure process is controlled by stress-induced fractures around the excavation zone, which are formed parallel to the excavation walls. In the case of an underground excavation where the magnitude of in situ stresses is relatively high, then slabbing, spalling and zonal disintegration are regarded as the main failure mechanism (Dowding & Anderesson, 1986; Martin & Christiansson, 2009; Feng et al, 2012). Thus, rockburst phenomenon is recognized as a specific type of rock mass failure around excavations in hard and brittle rocks and in high-stress environments (the yellow boxes in Fig. 1). Although rockbursts must have occurred in mines since the earliest days of underground mining, the first clearly reported cases date from the 18th century. A rockburst was first reported in a tin mine in Britain in 1738, and the first recorded rockburst occurred at a British coal mine in Stafford in 1938. The extreme level of rockburst were announced in 1900 in the Golden Horn area in India, which annihilated the buildings on the ground. Other such event of variable intensity and impact were reported from mines in Africa, Australia, Canada, China, Chili, Korea, Norway, Russia, Sweden, and the U.S., where important underground excavations and tunnels have been built (Lee et al., 2004; Liu et al., 2015; Ahmed et al., 2017). Rockburst hazard seriously endanger the safety of mine personnel, mine galleries and equipment. In addition, it causes major perturbations to mine development and operations, and can seriously impact on the economic performance of a mine or company. It is therefore primordial to control this issue in underground excavations.

As mentioned, the rockburst may now be a universal problem. The rockbursts usually occur in zones of high magnitude in situ stresses, in hard and brittle rocks. After excavation, the magnitude of in situ stresses and their orientations are perturbed and if the magnitude of induced stresses exceeds the rock strength, cracks are created in the rock and propagate around the underground excavation. Cracks in the rock make it more likely to lose its strength resulting in its failure. There is no consensus on the significant parameters which affect the trigger of a rockburst due to hidden nature of the geological conditions. Nevertheless, a number of research studies have achieved thoughtful and profound results on rockburst mechanisms and their prediction. Zhou et al. (2011) proposed that preexisting cracks in rock are beneficial to the sudden release of energy stored in rock masses. Lu et al. (2018) demonstrated that geological structures, such as faults and joints, bring about sharp stress increase, which may lead to a rockburst. Yang et al. (2017) indicated that high in situ stresses are the main factor that causes strain energy accumulation. Zhu et al. (2010)

proposed that a great importance should be attached to rockburst brought by dynamic disturbance during underground mining.

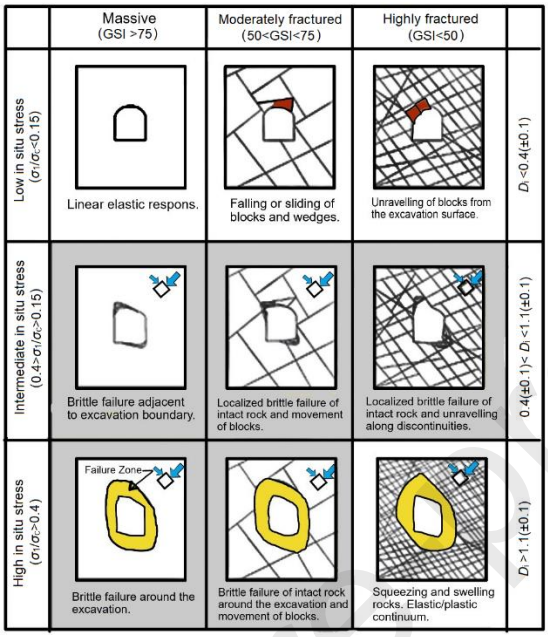

Fig. 1. Modes of rock mass instability as a function of GSI and the ratio of maximum far-field stress (Hoek & Brown, 1980).

As mentioned above, rockbursts cause substantial damages to underground structures and equipment, and they threaten workers' safety. Thus, this study reviews the global history of rockburst observation in underground excavation and represents some current definitions of rockburst. The recent rockburst classification systems and the underlying rockburst mechanisms are explained as well. Then, this study provides a brief literature review on strainburst, pillar burst, and fault-slip burst. The last part of this paper includes the introduction of empirical methods of rockburst based on stress and energy methods. Notably, this review paper is based on the utilization of empirical methods of rockburst prediction for several purposes, including the case studies and selection of numerical or intelligent methods.

2 Classification of Rockburst

Properly explaining the definitions of rockburst, classification systems, and their mechanism is essential before describing the rockburst prediction methods. As a simple definition of rockburst mechanism, an increase in the tangential stress (σ_θ) and a decrease in the radial stress (σ_r) will lead to the release of rock mass elastic energy and the occurrence of a sudden rockburst (Jiang et al., 2010). Several definitions of rockburst have been proposed from the first observation of rockburst at the Kolar gold mine in India and the British coal mine (Cai, 2016). Terzaghi (1946) firstly introduced the definition of rockburst as a sudden separation or falling off of the rock from the

tunnel wall due to excessive stress on brittle and hard rocks. Cook (1963) provided the second definition as an uncontrolled disruption of rock associated with a violent release of energy. Obert and Duvall (1967) reported rockburst as any sudden and violent explosion of rock when the amount of stress exceeds the strength of rock mass. They mentioned that rockburst occurs when the uniaxial compressive strength (UCS) of the rock is between 100 and 400 MPa and its elasticity modulus is between 40 and 90 GPa. Russenes (1947) stated that any kind of rock mass failure, such as spalling, ejection, and fracture face, is regarded as rockburst. Blake (1972) suggested that rockburst is a sudden separation and expulsion of rock from its surrounding due to the release of rock energy. Tan (1988) mentioned that not all rock failures are necessarily rockburst. Only the ejection of rock is a rockburst, and the other types of rock failure are due to the brittle fracture phenomenon. From 1980 to 2009, all rockburst definitions focused on the ejection of rock mass when the rock energy is released (Gill et al., 1993; Hedley, 1992; Tao, 1988; Kaiser et al., 1996; Ortlepp & Stacey, 1994; Singh & Goel, 1999; Wang & Park, 2001; Guo & Yu, 2002; Blake, 2003; He, 2005; Zhou et al., 2017). Dietz et al. (2018) defined rockburst as a sudden and violent movement of rock in high-stress environments. All definitions of rockburst seem to be based on the fact that the rock's elastic energy is suddenly released due to perturbation of the magnitude of in situ stresses during the excavation.

The objective of rockburst classification is to determine the rockburst mechanism in the underground excavation. Rockburst was first classified in 1950 based on its origin (Colson, 1950). Rockburst should be classified in different types based on its intensity, seismicity, the shape of the ejected rock, and others. The rockburst classification is generally categorized into three groups. The first one is a classification based on rockburst type (features of failure plane observed in underground excavation). The second is based on rockburst intensity, and the last one is based on rockburst's triggered mechanism and evaluation of seismic events (Kaiser et al., 1996; Ortlepp & Stacey, 1994). Kaiser et al. (1996) highlighted that changing rock massive volume, tunnel wall deformation, and rock-throwing intensity can be used as the three main criteria for the rockburst classification. In 1996, the rockburst classification included new phenomena: strainburst, slip/fault rockburst, and the combination of two mechanisms (Tang, 2000). Ortlepp and Stacey (1994) classified rockburst on the basis of the source and damage mechanisms. The advantage of this classification is that the type of rockburst was clearly defined on the basis of the energy source and damage mechanisms (Zhou et al., 2018). There are some differences between source damage and mechanism damage. The energy source provides sufficient energy for triggering the rockburst event. This energy can be provided by stored elastic energy in the rock or a seismic event. For example, buckling damage is due primarily to the strain energy stored in the "plates" subjected to buckling. Moreover, the location and source of damage can be coincident or not. In other words, when the location and source of damage are coincident, rockburst occurs in an area where energy was stored. In the case of buckling rockburst, the source of energy is elastic energy which is stored in the rock. However, when the location and source of damage are not coincident, the energy that triggers the rockburst may originate from a seismic event, in which the source of hypocenter may be some distance away from the damage location. For example, when a shear rockburst occurs the energy source may come from a blasting event located far from the location of the ejection damage. Regarding to classification of Ortlepp and Stacey (1994), the location and source of damage are

coincident for the first three classes (strain bursting, buckling, and face crush). However, in the last two classes, the rockburst mechanism includes a shear failure on a plane that could reach hundreds of meters (Ortlepp & Stacey, 1994). Table 1 represents the rockburst classification with respect to the seismic events in a tunnel.

Table 1 Classification of rockburst proposed by Ortlepp and Stacey (1994).

Seismic event	Postulated source mechanism	First motion from seismic record	Richter magnitude, *M*
Strain-bursting	Spalling rockburst with a severe ejection of fragments	Usually undetected, could be implosive	−0.2–0
Buckling	Outward expulsion of pre-existing larger slabs parallel to the opening	Implosive	0–1.5
Face crush	Violent expulsion of rock from the tunnel face	Implosive	1.0–2.5
Shear failure	Violent propagation of shear fracture through the intact rock mass	Double-couple shear	2.0–3.5
Fault-slip	Severe renewed movement on existing fault	Double-couple shear	2.5–5.0

Ortlepp and Stacey (1994) categorized rockburst into the four groups on the basis of the damage mechanism, namely, strainburst, buckling, ejection, and arch collapse. Strainburst likely occurs in massive rock masses rather than the jointed or fractured ones, where thin and very sharp edge fragments of the rock are violently separated from the rock mass. The orientation of in situ stresses and the geometry of excavation are significant factors in determining the location of fragments. Strainburst can occur when the magnitude of field stresses is as low as 15% of the UCS of rock (Singh, 1987). Thus, the occurrence of high-magnitude in situ stresses is not required for strainburst. From the observations of Broch and Sørheim (1984), the probability of rockburst in the form of strainburst increases as the rock mass strength increases. In addition, when a machine-excavated method is used, the probability of strainburst occurrence is more likely to be higher than when using the drill and blast methods. Chen et al. (2013) reported that the strainburst may cause the rocks to be brittle and non-brittle, such as limestone and shale. Moreover, buckling occurs anywhere around the perimeter of the excavation opening, depending on the type of geological structures. This mechanism likely occurs in transverse rocks. The stored energy in a massive rock mass can indicate the buckling potential, whereas some other sources of energy, for example, the wave of the blasting, can cause buckling. The ejection type of rockburst is defined as the ejection of the portion of tunnel hanging or footwall associated with the shock wave. The presence of joints or fractures affects the shape of the ejected block of rocks. The collapsed arch should be considered as the sub-level of the ejection type of the rockburst. This type of rockburst occurs at the geological structure or induced fractures. Figure 2 shows such types of rockburst.

.

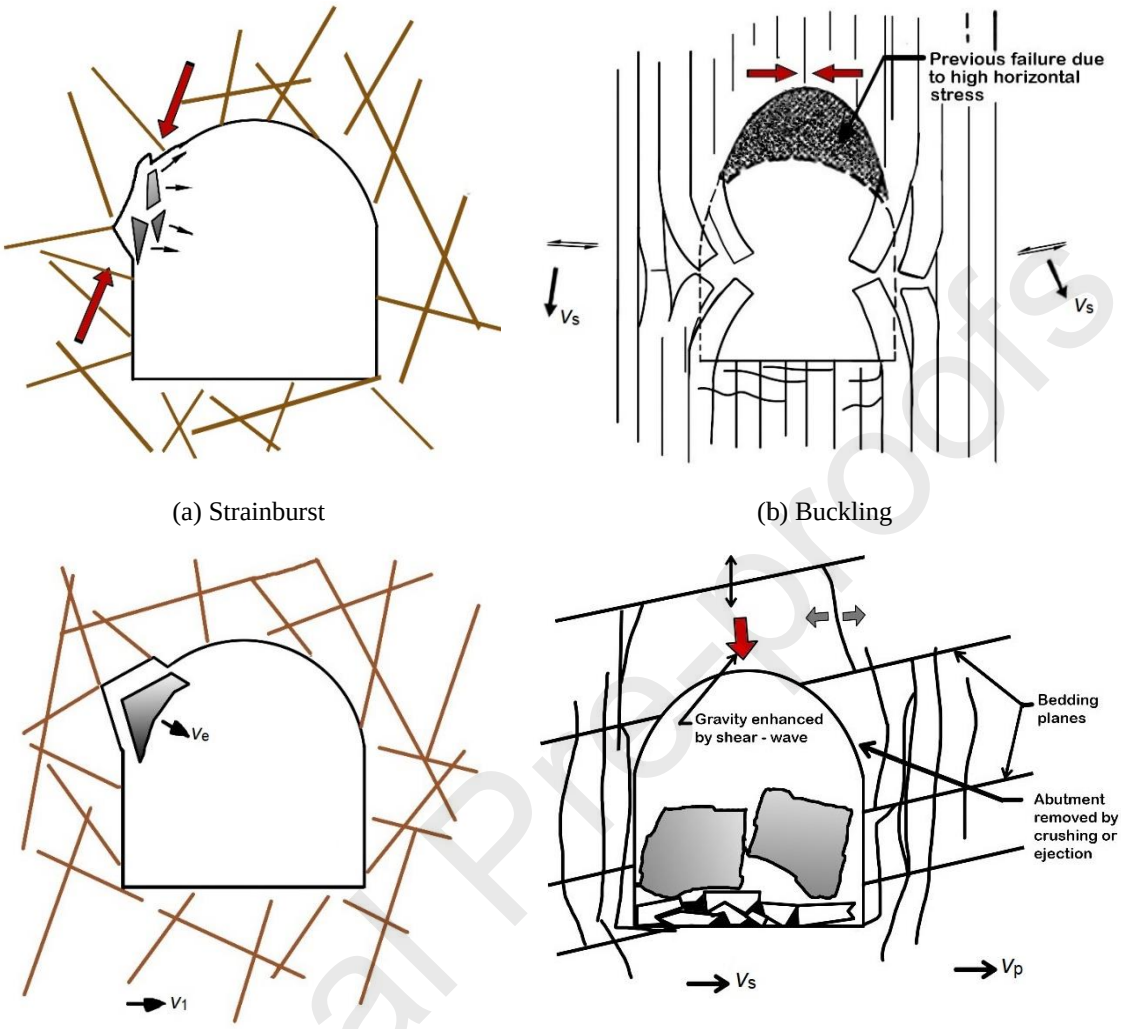

(a) Strainburst (b) Buckling

(c) Ejection (d) Collapsed arch

Fig. 2. (a) Strainburst, (b) buckling, (c) ejection, and (d) collapsed arch schematic (Ortlepp & Stacey, 1994).

Hedley proposed another rockburst classification system and classified it into three groups: (a) inherent burst, (b) induced burst, and (c) fault-slip burst (Table 2) (Hedley, 1992). However, this classification has significant disadvantages because the geomechanical nature of rockburst is not adequately considered, and this classification is not capable of describing the rockburst process mechanism.

Table 2 Classification of rockburst (Hedley, 1992).

Rockburst type	Definition
Inherent burst	Magnitudes of in situ stresses are high enough to cause failure in the initial step of excavation
Induced burst	The remaining stresses after the excavation on the pillar
Fault-slip burst	Existing major geological structure

Kaiser et al. (1996) proposed a rockburst classification based on self-initiated and remotely triggered mechanisms. The former refers to those that occur during the excavation; whereas, the latter refers to those that occur after the excavation by a dynamic load added up to the stored energy around the excavation area. Moreover, Kaiser (2009) proposed another classification of rockburst, namely, strainburst, fault-slip burst, and pillar burst. Misich and Lang (2001) defined another rockburst classification based on the time between the unloading and the start of the rockburst. This classification was also based on the source and damage mechanisms of rockburst. Tang (2000) considered three major types of rockburst, namely, strainburst, fault-slip burst, and the combination of the two mechanisms. The strainburst and fault-slip burst are likely to occur underground in a large and deep scale in the excavation area. However, he stated that the most common type of rockburst in a tunnel should be considered strainburst. He et al. (2015) mentioned that strainburst and pillar burst occur in a high-stress environment; whereas, the fault-slip burst occurs in major geological structures far away from the location of underground excavation. Recently, Li et al. (2017) proposed a highly comprehensive classification of rockburst. They used several geological and mechanical rockburst analyses in Chinese mines by considering the rockburst mechanism, severity, and type. Then, they proposed six geomechanical rockburst types based on the failure mechanism as follows: (1) tensile cracking and spalling, (2) tensile cracking and toppling, (3) tensile cracking and sliding, (4) tensile shearing and bursting, (5) buckling and breaking, and (6) arc shearing and bursting. Figure 3 depicts the aforementioned six types of rockburst. The rockburst mechanism will be discussed further in Section 2. As mentioned earlier, the basic classification system classifies the rockburst as strainburst and fault/slip burst. Hence, tensile cracking and spalling are referred to as strainburst, and tensile cracking sliding type is referred to as the slip/fault burst. The other four geomechanical types of rockburst, proposed by Li et al. (2017) cannot be regarded as either strainburst or slip-fault burst due to the combination of initial crack mechanism and the development of micro-cracks in intact rocks. Table 3 shows the properties of six geomechanical types of rockburst.

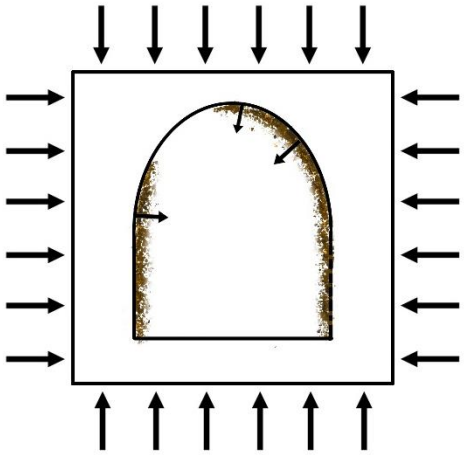

(a)

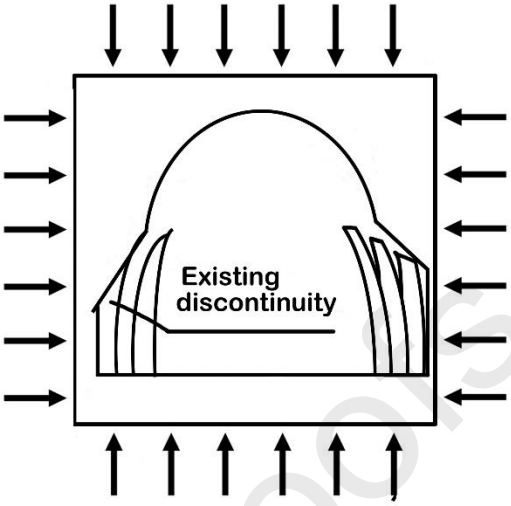

(b)

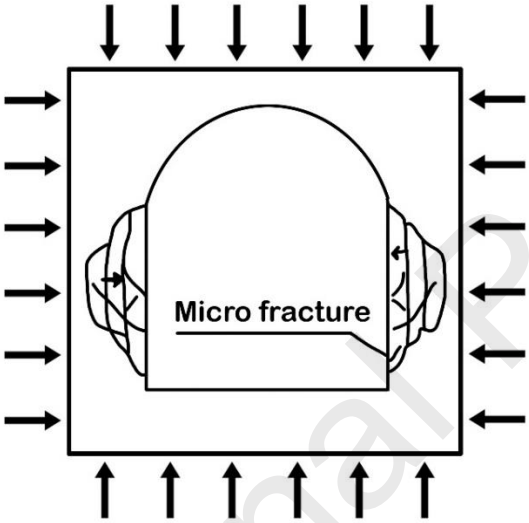

(c)

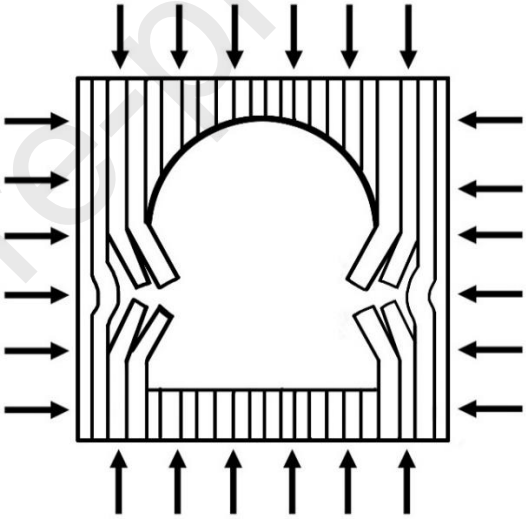

(d)

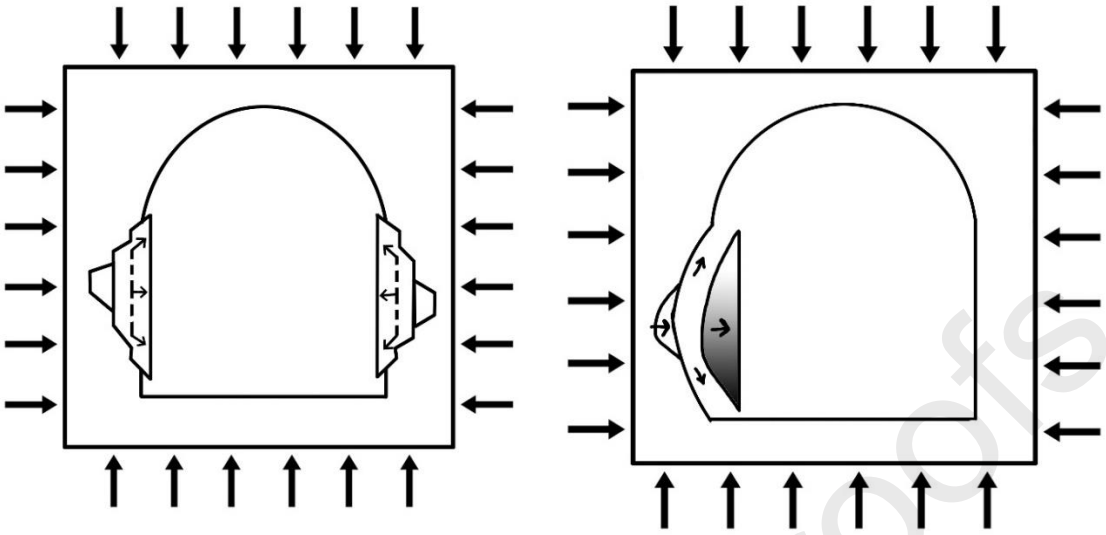

(e) (f)

Fig. 3. (a) Tensile cracking and spalling, (b) tensile cracking and toppling, (c) tensile cracking and sliding, (d) buckling and breaking, (e) tensile shearing and bursting, and (f) arc shearing and bursting (Li et al., 2017).

Table 3 Rockbursts and their properties (Li et al., 2017).

Characteristic	Tensile cracking and spalling	Tensile cracking and toppling	Tensile cracking and sliding	Buckling and breaking	Tensile shearing and bursting	Arc shearing and bursting
Structure of rock masses	Existing micro-fractures parallel to the free surface	Layered structure	Layered or massive with an existing fracture zone	Layer or layer-like	Intact or massive	Intact or massive
Cracking property	ensile	Tensile	Tensile and shear	Tensile	Tensile, shear, and tensile-shear	Tensile and shear
Failure plane	Flat or conchoidal with step-like boundaries	Irregular or stepped	Stepped or curved	Stepped or conchoidal	Stepped or arc-like	Elliptical or dome-like
Energy release	Negligible	Little	Moderate	Moderate	Large	Large or very large

As mentioned earlier, the other rockburst category is based on intensity. The intensity grade varies from low to high; however, these grades would be different for each classification. Russenes (1974) proposed the first classification based on the severity of rockburst and categorized the rockburst into four groups: none, weak, moderate, and severe rockburst. Tan (1992) also proposed another rockburst classification system based on the intensity, where many laboratory tests were conducted considering the geomechanical characteristic and the failure type and shape. Thus, the rockburst magnitude was classified into none, weak, moderate, and severe. Moreover, Brauner (1994) proposed a rockburst classification system with three categories based on the extent of rock destruction. Kaiser et al. (1996) found that rockbursts could be classified into minor, moderate, and major groups. According to this study, the intensity of rockburst should be derived from empirical evidence, the depth of the damage zone in the rock mass, and geometric considerations. Chen et al. (2013) proposed a quantitative rockburst evaluation method based on the radiated energy of rockburst, which could be recorded through microseismic technique. Zhang and Dai (2017) proposed four rockburst intensity grades, from grade I (no intense) to IV (extremely intense rockburst) based on the index distance and uncertainty measure.

In coal mines, coal-gas explosion represents an extra type of rockburst that can cause serious dynamic disasters in deep mining (Li et al., 2015; Zhu et al., 2016). Coal-gas outbursts and rockbursts usually occur independently. However, increasing mining depth in recent years has caused these two dynamic disasters to coexist, be mutually induced, and combined, resulting in

new types of dynamic disasters called coal-gas compound dynamic disasters (Pan, 2016; Sun & Li, 2011).

Asvershin (1959) studied the question whether gas explosions cause rockbursts, or rockburst causes gas explosions, or whether both can occur at the same time. Shepherd et al. (1981) classified coal and rock dynamic disasters into the coal and gas outbursts, bumps or rockburst and outburst from the floor or roof strata. The international classification of coal and rock dynamic disasters developed by Dechelette et al. (1984) comprises coal (rock) and gas outbursts, gas outbursts, rockbursts, and mine tectonic phenomena. Zhang (1991) studied the mechanisms of coal and gas outbursts, and rockbursts, established the occurrence criteria for each disaster, and then developed the unified stability-losing theory of the two types of disasters. Li et al. (2005, 2007) discussed how coal-gas outbursts are induced by rockburst and developed the correlation between rockburst and gas outbursts in deep mining. As a result, they suggested high gas pressure would play a very significant role in the triggering of a rockburst. Fisher (2013) investigated the effect of gas emissions on rockburst. As he pointed out, high-pressure gas triggers rockbursts by extending the plastic disturbed zone. Cao et al. (2015) developed an evaluation system for coal and rock dynamic disasters, in which the dynamic disasters are divided into typical and atypical disasters based on the unified energy equation and the concept of degrees of gas participation in coal and rock dynamic disasters. Typical dynamic disasters are coal and gas explosions and rockbursts, while atypical dynamic disasters are coal-gas impacts and coal-gas extrusions. In the case of atypical dynamic disasters, burst tendency is the primary classification indicator. If the coal samples burst, the type of disaster is coal-gas impact, otherwise, it is coal-gas extrusion. Compound dynamic disasters may also exhibit a low index phenomenon, that is, coal and rock without burst tendency may still produce a rockburst disaster under the influence of gas outbursts. Pan (2016) classified coal and rock dynamic disasters according to the relative release of gas internal energy and coal-rock elastic energy as follows: coal and gas outburst, outburst-rockburst compound disaster, and rockburst compound disaster. Such classification represents a significant improvement relative to the previous classifications. However, compound dynamic disasters are determined by the relative amount of two energy types released, without considering the order in which the energy types are released, which does not allow to take into account mutual induction and mutual transformation between coal and gas outburst and rockburst. The researches of Fisher (2013) and Li et al. (2015) show that the expansion energy of high-pressure gas desorption has a positive effect on triggering rockbursts. Therefore, it appears that a gas outburst can induce or increase the likelihood of a rockburst, which is caused by the dynamic energy released from the gas pressure, leading to a new classification of coal and rock dynamic disasters as follows: (1) Rockburst-induced outburst dynamic disaster means that (coal and) gas outburst is induced by the rockburst in a short time; (2) Outburst-induced rockburst dynamic disaster means that rockburst is induced by the (coal and) gas outburst in a short time; (3) Outburst and rockburst coupling dynamic disaster means that (coal and) gas outburst and rockburst occur at the same time and coexist each other (Wang & Du, 2019). There is no indication of a chronological sequence between these events.

Besides classification of coal and rock dynamic disaster, there is another phenomenon known as coal bumps. This is a dynamic phenomenon, which will cause sudden and severe damage to underground mining. It basically involves the release of elastic deformation energy from the

surrounding rock mass of a mining tunnel, characterized by loud noises and the projection of large quantities of rock or coal mass. In general, coal bumps are characterized by the following features: (1) There are no clear macro-precursors to coal bumps; (2) They cannot be predicted in terms of magnitude, location, and likelihood of occurrence; (3) Other dynamic disasters can also co-occur, such as gas eruptions, gas explosions, and water inflow (Jiang et al., 2014). Phillips (1944) categorized the coal mine bumps as either pressure or shock bumps. A pressure bump occurs when a strong or brittle pillar in a developed area is statically stressed past the failure strength of the coal. A shock bump is caused by dynamic loading of the coal through either dramatic change in the stress distribution within the overlying strata or by an abrupt loading of the coal ahead of the face resulting from dynamic roof rock failure. Spalding (1948) explains that certain types of rock bumps can be classified as ring, shear, or pillar bumps. Holland (1954) indicated that many shock bumps in a mine were actually caused by coal mined under high static loads. As a result of this study, bumps previously thought to be caused by dynamic loading are actually the result of local variations in mine geology and coal properties or improper mine design and sequencing, which created zones of high stress. Zanski et al. (1964) concluded that bumps are classified into seam, roof, and floor bumps based on where they occur. According to Qian & Zhou (2011), coal bumps can be divided into sliding coal bumps resulting from fault slips and strain energy bumps resulting from coal mass failures. In terms of geological conditions specific to a site, coal bumps can be classified into three categories based on their patterns and associated factors (Jiang et al., 2017): **Type I**: Material failure is the cause of coal bumps. Cracks can form, develop, spread, penetrate, and propagate during the excavation of tunnels or longwall panels. As the surrounding rock or coal mass reaches its maximum strength, coal bump can occur. **Type II**: Coal bumps are caused by hard roofs or floors. There can often be large stiffness differences between roof/floor strata and coal seams when coal bumps occur (Rostami et al., 2015). During mining, the hard roof or floor may release accumulated strain energy instantly. The coal may develop coal bumps or move horizontally toward the tunnel in this case. **Type III:** Coal bumps are caused by tectonic structures. During the long-term evolution of rock strata characterized by strong tectonic structures, a huge amount of elastic energy can accumulate in the regions adjacent to the tectonic structures. Mining nearby may also reactivate faults, resulting in coal bumps. In practice, high in situ stress may result in fault reactivation, release of high pressure and coal bumping as mining proceeds. The degree of damage caused by coal bumps of Types II and III is greater than that caused by Type I. (Jiang et al., 2017).

As mentioned before, the classification of rockburst evaluates not only the intensity of rockburst but also the type and shape of the failure zones. However, obtaining additional information about the mechanism of rockburst provides complete and comprehensive information on the rockburst issue in the underground excavations. In the next section, the mechanism of rockburst will be discussed and reviewed.

As the discussion on this section, rockburst classification is typically used to determine how they occur. Several distinct types of rockbursts have been identified based on the rockburst phenomenon, the rockburst mechanism, the rockburst energy and stress, the scale and location of rockbursts, and the cause and effect of rockbursts. Rockburst classification methods such as those mentioned above have been widely used by mining and geotechnical engineers owing to their simplicity and flexibility. However, even when they share the same methodology, the different evaluation indices

can generate results that are conflicting. Rockbursts were first classified based on shape and rock-projection intensity, such as the classifications by Russenes (1974), Brauner (1994), Tan (1992), and Kaiser et al. (1996). One shortcoming of such classifications is that they do not consider underlying mechanisms, seismic events, and rockburst shape. Furthermore, there is no sufficient information about fault slip burst. The classification of Kaiser et al. (1996) has the advantage of considering two significant mechanisms of rockburst, such as self-initiated or remotely triggering, as well as its intensity. More recent classifications are based on the idea that rockburst events should be categorized based on the mechanism and severity (e.g., Tang, 2000; Kaiser, 2009; He et al., 2015). One of the best rockburst classifications, by Li et al. (2017), defined six classes of rockbursts and their mechanisms. The advantage of that classification is that the different types of rockburst are described according to their failure plane, type of cracking (tensile or shear), and amount of energy released. By combining this classification with mine staff observations and the recorded seismic data of a mine, the best classification of rockbursts can be determined for a mine site. Moreover, according to this classification of rockburst, it is possible to categorize rockburst predictions into two categories: short-term ones, which can be used during the life of a project, and long-term ones, which are useful at the design stage. The short-term prediction of rockbursts primarily relies on field monitoring but also includes micro-seismic, electromagnetic, drilling cutting, micro-gravity, and infrared thermal imaging. After underground development is complete, short-term rockburst prediction methods can be used. It is only possible to install monitoring equipment in underground excavations after tunneling or drifting underground. The design stage of future excavations should use a long-term rockburst prediction method in order to avoid areas with high rockburst hazard during excavation. A long-term rockburst prediction is based on both rockburst potential and field conditions. Scholars have proposed several indicators to best evaluate burst potential. These methods will be discussed in Section 4.

As robust and complete a classification schemes can be, rockbursts evaluation and classification depend on engineers' evaluation and access to data for each specific case (e.g., length, shape, and intensity) and there is a human factor that cannot be eliminated in classifying rockbursts. This implies that a similar environment or event may lead to different measures depending on how the classification was made, and by whom. Thus, the proposed method for unified rockburst classification needs to be implemented in future research.

3 Rockburst Mechanism

When the accumulated strain energy exceeds the energy storage limit of the rock mass, excessive energy will be released suddenly, and the rock mass around the opening will be violently ejected from the rock mass domain, as shown in Fig. 4.

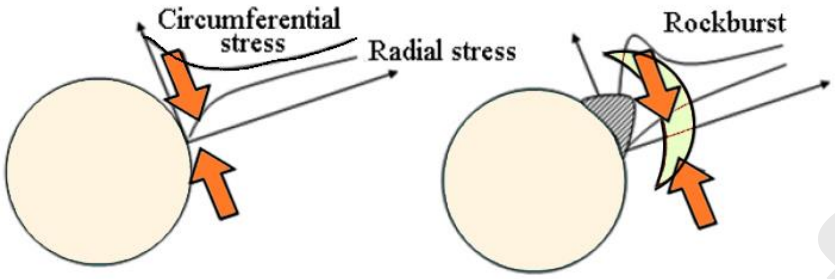

Fig. 4. Schematic sketch of rockburst (Zhang et al., 2003).

The aspects of rockburst mechanisms are defined by two main mechanisms: damage and source mechanisms. The latter causes the seismic event, and the hypocenter of the source mechanism can be far away from the location of the damage. The former directly causes the damage, and its location is identical to the damage site (Ortlepp & Stacey, 1994). From the studies in the Canadian hard rock mines on rockburst hazards, the rockburst damage mechanisms depend on the level of underground confinement (Kaiser et al., 2000). Accordingly, the rockburst mechanism could be classified into three groups, namely, strainburst, pillar burst, and fault-slip burst. Strainburst occurs under low-confinement conditions (reducing the radial stresses and increasing the tangential stresses), whereas the pillar burst occurs at the boundary between low and high confinement conditions. Moreover, the fault-slip rockburst occurs in high confinement conditions. Figure 5 shows the classification of rock mass failure modes developed based on the level of underground confinement. The above-mentioned modes of underground instability and their corresponding desired occurrence conditions (low and/or high confinement conditions) are in accordance with the elementary rockburst classification proposed by Board (1996).

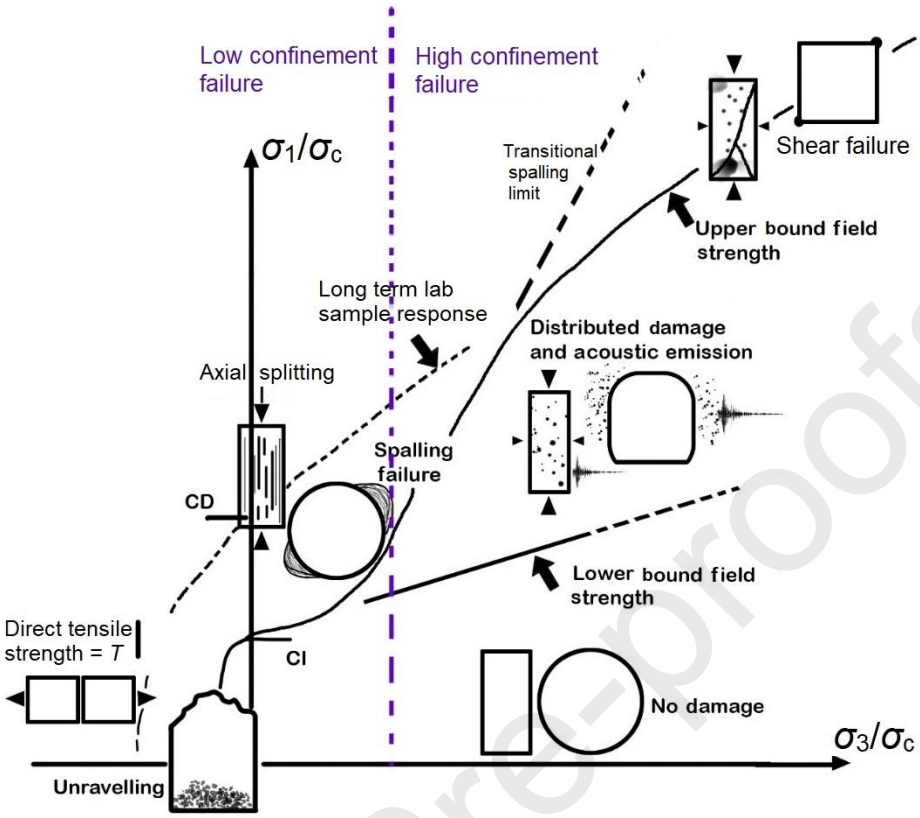

Fig.5. Rock mass failure modes under low and high confinement (Diederichs, 1999).

3.1 Strainburst

As mentioned before, the rockburst is classified into three groups, as shown in Fig. 6 (Castro et al., 2012). Rock mass damage at low-confinement conditions can be generally divided into two categories: (1) stress-induced failure with slabbing and spalling failure plane and (2) structurally controlled gravity-driven failures (Kaiser et al., 2000). However, the first group is demonstrated as strainburst depending on the range of deviatoric stresses. According to the strainburst mechanism (decreasing the radial stress and increasing the tangential stress), rock mass failure develops on the perimeter of the excavation under low-confinement conditions. Under a low-confinement condition, the fractures intend to extend in the direction of the major induced stress and develop sub-parallel to the excavation boundary when the rock is exposed to the compressive loads (Diederichs, 1999). Strainburst likely develops by the stress-induced spalling and slabbing failure. An important characteristic of strainburst is that no damaging vibration occurs prior to rock failure. Damaging vibration is generated during and after bursting. The deviatory stress level was defined to evaluate the strainburst severity and rock mass damage around the excavation zone (Castro et al., 2012), as shown in Table 4.

Table 4 Likelihood of strainburst based on the level of deviatoric stress (Castro et al., 2012).

$\sigma_1 - \sigma_3/\mathrm{UCS}$	Rock mass damage	Likelihood of strainburst

0.35	No to minimum	No
0.35–0.45	Minimum	No
0.45–0.6	Moderate	Minor
0.60–0.7	Moderate to major	Moderate
>0.7	Major	High

Notably, the deviatoric stress only considers the induced principal stresses and the UCS of intact rock. However, the ground stress cannot represent the potential energy release driven by the loading system, given that the potential energy release depends on the loading stiffness (loading stiffness is the degree to which an object resists its deformation in an applied load) (Duan et al., 2019).

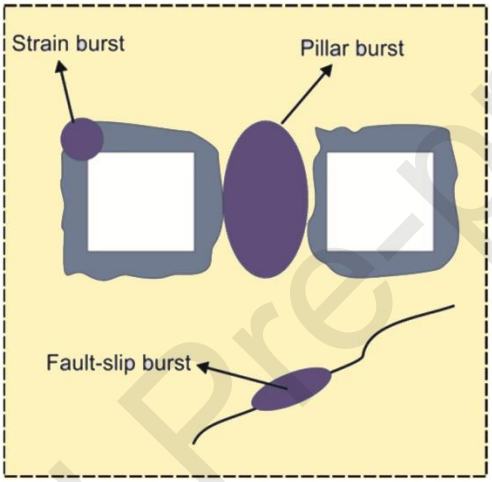

Fig. 6. Schematic representation of rockburst potentials (Castro et al., 2012).

3.2 Pillar burst

In deep underground hard rock mines, pillars have the potential to cause rockburst because of the high strain energy stored within them and the brittle characteristics of the rock mass (Sainoki & Mitri, 2017; Hauquin et al., 2018). Pillar burst occurs under a low to moderate confinement condition (Fig. 7). Based on the pillar's width to height ratio (*W*/*H*), several confinement conditions develop in its core. With low *W*/*H* (approximately < 1.0), no or little confining stress is developed within the pillar. The confining stress increases as this ratio increases, resulting in two failure processes: surface spalling along the skin of the pillar and in the core of the pillar. The first mechanism is related to the occurrence of strainburst around drifts and stopes, and the second one is related to the development of short tensile cracks and their subsequent coalesce along the plane of induced shear stress. Many informative articles about the mechanism and effect of several parameters on pillar bust exist. However, these articles only focused on the strainburst and fault-slip burst.

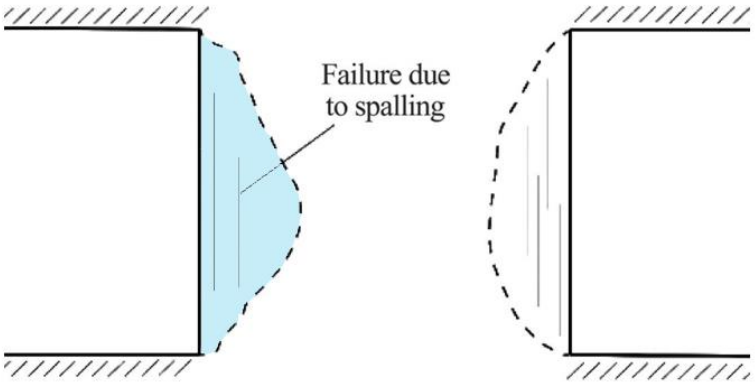

Fig. 7. Schematic of pillar burst (Sainoki & Mitri, 2017).

3.3 Fault-Slip Rockburst

Fault-slip or shear burst occurs under high confinement conditions and is triggered by stope extraction, drift development, and production blasting, which reactivated the pre-existing faults or formed the seismically active structural zones. The determination of strainburst or pillar burst is less complex than that of the fault-slip burst due to two main reasons. First, the determination of the physical and mechanical properties of the fault surface through laboratory and numerical studies could be very challenging. Second, the evaluation of stress re-distribution around the excavation opening could be a complicated task. Several friction models of fault-slip have been proposed to simulate the dynamic behavior of shear sliding, such as static-dynamic friction, velocity-dependent, slip-weakening, and rate and state-dependent models, to find a way to obtain the properties of fault (Sainoki & Mitri, 2014). Moreover, four vital factors can affect fault-induced slip in underground excavations. The first factor is called unclamping, which occurs on two scales: (1) the local unclamping as a result of overlapping the induced tensile stress field with a nearby pre-existing geological fault and (2) the regional unclamping, which occurs when the extension and size of mining excavation are sufficiently large. The difference between local and regional unclamping is that in regional mechanisms, slip is far away from the free face. The second important factor is daylight, which becomes vital when the actual underground excavation intersects a geological fault. In this situation, enough surface is provided for the fault to move toward the excavation area, and a considerable amount of energy is released, which could be accompanied by a large seismic event. The other important factor is stress rotation caused by perturbation of in situ stresses after excavation. In this situation, the major induced stress can switch from normally orientation to parallel with the fault plane. Finally, pillar shear is the last vital factor that contributes to fault-slip. Pillars can inhibit the displacement of the rock mass on one side of the fault and can also move freely on the other side. However, the dynamic behavior of fault-slip burst has not been fully understood, because the effect of physical characteristics of faults and the uncertainty of scale effect have not yet been completely investigated. Vasak et al. (2004) reported that the majority of microseismic events during mining excavation did not occur immediately after the stope excavation. Dowding and Andersson (1986) reported that with the increasing depth of excavation and the width and area of production face, the possibility of fault-slip burst also increases. However, the shear bursts occurred along with a new or major pre-existing geological structure. Zhang and

Fu (2008) used a continuous numerical model to analyze the effect of the fault on the occurrence of rockbursts in the tunnel. Sainoki and Mitri (2014) proposed dynamic modeling of fault-slip with Barton's shear strength. To this end, Barton's shear strength was inputted into the FLAC3D to analyze the effect of the fault-slip on underground excavation. The results demonstrated that the fault roughness has a significant effect on the seismic events. The chance of seismic events increases as the fault surface roughness increases. Moreover, the fault surface roughness affects the seismic moment and radiated energy. Sainoki and Mitri (2016) conducted a numerical analysis on dynamic behavior of fault in underground mines. The results showed that the fault friction angle has a significant effect on the maximum dynamic shear displacement during the stope excavation process, including the mining depth and position of fault with respect to the orebody. However, the stiffness and dilation angle of the fault shows no significant effect on the maximum dynamic shear displacement. Moreover, the fault position and friction angle have an influence on the seismic moment and the released energy of fault-slip. Then, they employed the finite-difference code of FLAC3D to conduct a numerical evaluation of fault-slip bursts using stress waves generated by stope production blast. Based on the obtained results, the reduction of normal stress on the fault is beneficial for the fault to slip over the fault plane. Furthermore, the blasting sequence has an important effect on the seismic moment and the released energy during the fault-slip. Meng et al. (2016*)* studied the prediction of fault-slip burst by using the experimental method. Based on the obtained results, the normal stress increases as the b-value decreases (the b-value reflects the proportion of large-magnitude earthquakes relative to small-magnitude ones). Hence, the risk of the rockburst induced by dynamic shear failure increases. A lower b-value is associated with a high rockburst probability and intensity. Sainoki et al. (2017) investigated the relationship of the fault-slip potential with the shearing of fault asperities. The numerical modeling was utilized (by FLAC3D software) to understand the relationship between the *D* and *H* parameters of an excavation area (*D* is the distance between the fault and orebody, and *H* is the height of the mined-out core). The results indicate that the potential for fault-slip burst drastically increases by increasing the value of *H*. Moreover, the potential of fault-slip burst does not increase when *D* is small because the entire accumulated strain energy is released when the distance between the fault and orebody is shortened. Moreover, the seismic moment and radiated seismic energy increase when the ratio of *D* and *H* decreases. Then, they estimated the extent of damage around an underground opening induced by seismic waves from mining fault-slip. To this end, the failure of rock mass under biaxial stress condition was considered, and the model examined ran under static and dynamic conditions. Two methodologies were applied to assess the extent of damage caused by the seismic wave propagation. The first one is the ratio of plastic strain increment to elastic strain limit, and the second is a variation of plastic strain energy density. Moreover, effective sheer and volumetric strain increment were tested. According to the results, volumetric strain increment is adequately accurate in determining the extent of damage near the stope wall; whereas, the effective shear strain can be used to estimate the extent of damage in the backfill. Moreover, the damage assessment method with plastic strain energy can be applied for detecting damage in an extensive area caused by seismic waves and fault movements. Furthermore, Sainoki et al. (2017) studied the characterization of a seismic fault-slip through numerical modeling and the influence of mining activity on the reactivation of a footwall fault. They demonstrated that the volume of ore extracted

before mining activity significantly affects the degree of clamping of the fault. They also showed that the shear movement on the fault is not the only cause of rockburst. The main reason is the stress changes induced by the slip. Meng et al. (2017) studied the significant factors affecting the fault-slip burst in deeply hard rock tunnels. The inherent properties of rock, such as strength and brittleness, and external environmental conditions, such as the magnitude of in situ stresses, dynamic disturbance, excavation sequence, and geological structure, influence the intensity of rockburst. Three different samples were examined, and the influences of the rock type, the normal stress, the surface morphology, the infilling, and shear history on fault-slip rockburst were investigated to evaluate these factors. The results show that rockburst occurs rapidly under following granite joint scenarios: stress drops after the peak stress and during the stick-slip period. In addition to the stress drop after the peak, stress and average stress drop during stick slip represent a linear relationship with normal stress. The value of average stress and stress drop increases with increasing the normal stress, which is associated with increased probability and intensity of fault burst. Moreover, they showed that the surface morphology also affects the intensity of fault burst. Another important result is the reduced probability of fault burst due to release of energy with reducing previous shearing events. One of the significant issues in underground excavation is the control and prediction of rockburst. The prediction methods are usually employed to decrease the rockburst damage to the tunnel or excavation zone. The prediction methods are often used for the strainburst rather than the pillar burst or shear burst, because the geological and geomechanical parameters of rock can be extracted easily for the prediction of rockburst than that of pillar burst or shear burst. The numerical analysis is normally used to analyze the pillar burst and shear burst. In general, the prediction methods are classified into the experimental, empirical, intelligent, and analytical methods. In this study, the empirical methods of rockburst prediction will be classified into three groups: stress, energy, and other methods of rockburst prediction. The other classification methods are referred to as the methods that are less important in the application for predicting rockburst in underground excavation or they have several indicators for rockburst prediction. As a brief description of the next section, the empirical methods of rockburst prediction will be explained, and the rockburst criteria with their corresponding definitions will be represented. Then, a comprehensive review of literature on the rockburst prediction methods will be presented.

3.4 Mechanism of coal- gas compound dynamic disasters

According to the classification of coal-gas compound dynamic presented in Section 2, and to understand the mechanism of coal-gas compound dynamic disasters in a systematic way, it is necessary to clarify all aspects of each classification that was proposed by Wang and Du (2019). In coal and rock dynamic disasters, energy dissipation and release play a major role. Therefore, energy dissipation can be used to explain mechanisms of dynamic disasters.

3.4.1 Mechanism of rockburst-induced outburst dynamic disaster

After a rockburst occurs, the elastic energy released from the burst acts as kinetic energy, promoting the development of cracks and fissures in gas-containing coal (Brady & Brown, 1993). Gas desorption and expansion occur simultaneously. In the absence of sufficient gas pressure, gas expansion energy is insufficient for the ejection of coal and it simply refers to the occurrence of gas outburst (abnormal emission). However, coal is prone to spall fracture under conditions

of higher gas pressure. The coal and gas outburst occurs when a large amount of desorption gases accumulate in fractures and eventually burst in the form of a pressurized storm when they come into contact with broken coal. In contrast, after the occurrence of rockburst, the stress state of coal changes, with cracks and fissures expanded, resulting in reduced ability of coal to resist deformation (Jiang et al., 2017). In addition, crack growth increases the stress potential of coal. In consequence, the coal body is more likely to attain the unstable state of outburst, increasing the likelihood of a coal and gas eruption.

3.4.2 Mechanism of outburst-induced rockburst dynamic disaster

By assuming that the outburst is triggered by mining disruption at a certain time, the outburst may induce rockburst by a number of ways:

(1) Outburst disasters involve desorption and expansion of gas, as well as failure of a coal or rock structure, which releases energy similar to mine seismic energy and the stress waves will be generated as a result of this transmission of energy. Due to the disturbance of the propagation medium caused by the stress wave, this process is regarded as that of dynamic loading. Whenever the stress wave interacts with the surrounding rock, it increases the load of the rock. As a result of the propagation of internal cracks and friction sliding between floor and roof, the surrounding rock loses its bearing capacity, eventually resulting in a failure.

(2) Coal bodies are thrown out with the subsidence of the roof during an outburst disaster, which results in further instability of coal and rock mass. With the redistribution of surrounding rock stress, the limit storage energy of the coal-rock system is reduced; meanwhile, elastic energy is transferred and released. In conjunction with the above factors, the unstable equilibrium state of the coal-rock deformation system is intensified, which may cause the roof rock to rupture and collapse, causing a rock burst.

(3) The coal-gas two-phase flow from an outburst hole is ejected at a certain velocity after an outburst disaster. In the tunnel space, the gas can be impacted and disturbed. Consequently, the coal and rock may become unstable due to the impact of airflow.

3.4.3 Mechanism of outburst and rockburst coupling dynamic disaster

Both coal and gas outbursts can happen in coal mines in addition to rockbursts. Unstability created by mining activity or natural events can induce the release of elastic energy leading to such bursts. Desorbed gas accumulated in the pores and fissures of coal has tensile destructive effects and spurts with broken coal into a pressurized storm, which results in the coal and gas explosion. A combined dynamic disaster can happen if coal and rock are elastically deformed and gas is stored and released simultaneously, with outburst and rockburst coexisting and combining.

4 Rockburst prediction methods

Rockburst prediction has always been a challenge worldwide and is one of the most significant ways of preventing and controlling rock failure in underground openings or tunnel excavations (Li et al., 2017). Different methods for prediction of rockburst have been studied since 1960. Up to this

date, researchers try to develop, modify, and verify the prediction methods through experimental tests, numerical modeling, and intelligent methods. The rockburst prediction methods are classified into three main groups: (1) regional, (2) local, and (3) current prediction. Regional prediction indicates the likelihood of rockburst based on the natural conditions of rock. The lithology of the strata, physical, and mechanical properties of the rock mass, depth, thickness and layer dip, and structural and tectonic patterns are the significant contributing factors. The local prediction can be used in regions within the rock mass, which are subjected to rockburst risk. Depth and thickness of rock mass and the influence of previous mining activities, such as pillar remaining and rib edges, are the significant factors of local rockburst prediction (Ptáček, 2017). The current prediction is defined as the activities performed in underground mining to determine the regions of strata with a stress concentration (Talka et al., 2005). Prediction methods can also be classified into analytical, experimental, intelligent, laboratory, and numerical methods. Empirical methods of rockburst prediction are divided into two main groups, namely, the stress and energy methods. The former refers to those methods that consider the magnitude of induced stresses and the geomechanical parameters of rock. By contrast, the latter refers to those methods which consider the stored elastic energy of rock mass (Cook, 1963). The empirical methods rank the rockburst based on the intensity level as no, light, medium, and severe or strong rockburst. No rockburst resembles the condition within which no sounds of rockburst and no rockburst activity are expected to occur. Light rockburst is used where the surrounding rock mass is deformed, cracked, or rib-spalled, and a weak sound or no ejection phenomenon exists. Medium rockburst defines the conditions where the surrounding rock mass is deformed and fractured, and a considerable number of rock chips are ejected. In these cases, a light and sudden destruction occurs, accompanied by crisp crackling often in surrounding rock. Last, severe rockburst is considered in situations where the surrounding rock mass bursts severely and is ejected suddenly into the opening void, accompanied by a continuous strong burst, roaring sound, air spray, and storm phenomena. Moreover, a rapid expansion of rockburst to the depth of surrounding rock is expected to occur. In the following sections, all the stress and energy methods of rockburst prediction will be reviewed. These methods will be explained, and their application and importance in prediction of rockburst in underground excavations will be studied.

4.1 Stress Methods

Empirical stress estimation constitutes the most widely used category of methods for rockburst prediction and prevention in underground mining; it employs various indices and indicators to characterize the rock mass. The geomechanical parameters of intact rock and the magnitude of in situ or induced stresses are key factors indicating the severity of rockburst in such methods. These methods have shown to be easy to use while making an acceptable rockburst prediction in deep underground environments (Gong & Li, 2007).

Some very early observations can help get an idea of rock mass properties such as drill core description. For example, core discing represents a useful source of information to estimate and locate potentially overstressed areas. The pre-loading of a rock mass has consequences on rock stress evaluation. As a result of boring holes to obtain cores, stress concentrations occur directly at the coring bit/rock interface. When the core is drilled, the annular groove causes the in situ stresses

to redistribute, leading to high induced stresses throughout the core. A core can thus be significantly damaged because of the sudden release of that stress, which can further be exacerbated by rock anisotropy. High in situ stress and brittle rock can result in 'core discing', where the core appears as thin 'poker chips'. In extreme cases, the discs can become so thin that they resemble *milles feuilles*, or *flaky pastry*. The presence of discing in cores is often interpreted as evidence for high-stress zones (Fairhurst, 2003). Understanding overstressed areas could enable us to consider that the rockbursts are perhaps more likely to occur in specific areas. Let us now turn our attention to stress methods and rockburst prediction. The most common empirical stress methods and their applications are reviewed as follows.

4.1.1 Rock Brittleness Coefficient

Brittleness of rock, as one of the significant properties of rock, is considered an index to determine the intensity of rockburst in an underground excavation. From a mechanical point of view, brittleness is a reduction of strength derived from the bond between the grains. According to the experimental results and site investigation, the rock brittleness coefficient is defined as the ratio of UCS to the tensile strength of intact rock as follows (Qiao & Tian 1998; Chen et al., 2013):

$$B_{\mathrm{i}} = \frac{\sigma_{\mathrm{c}}}{\sigma_{\mathrm{t}}}, \qquad (1)$$

where σ_{c} is uniaxial compressive strength of the rock and σ_{t} is tensile strength of the rock. The both values are in MPa.

Table 5 Rockburst intensity based on the brittleness coefficient (Wang & Park, 2001).

Rock Brittleness Coefficient	Risk of violent rupture
No rockburst	$B_{\mathrm{i}} > 40$
Weak rockburst	$26.7 < B_{\mathrm{i}} < 40$
Moderate rockburst	$14.5 < B_{\mathrm{i}} < 26.7$
Strong rockburst	$B_{\mathrm{i}} < 14.5$

Moreover, Zhang et al. (2003) mentioned the other classification of rockburst based on the rock brittleness coefficient (Table 6). Based on their classification, the possibility of rockburst increases as the rock brittleness coefficient ratio increases.

Table 6 Rockburst intensity based on the brittleness coefficient (Zhang et al., 2003).

Rock Brittleness Coefficient	Risk of violent rupture
No rockburst	$B_{\mathrm{i}} < 10$
Weak rockburst	$10 < B_{\mathrm{i}} < 18$
Strong rockburst	$B_{\mathrm{i}} > 18$

In terms of accumulated energy, the brittle deformation coefficient (K_u) is defined as:

$$K_u = \frac{U}{U_t}, \quad (2)$$

where U is the total peak strength of rock before rock deformation (in %), and U_t is the permanent deformation of rock before the peak or elastic deformation (in %) (Neyman, et al., 1972). Moreover, brittle deformation coefficient is defined as the ratio of the tensile strength of rock to the maximum in situ stress component as follows:

$$K_u = \frac{\sigma_t}{\sigma_1}. \quad (3)$$

Table 7 shows the intensity of rockburst based on the brittle deformation coefficient.

Table 7 Rockburst intensity based on the brittle deformation coefficient (Neyman, et al., 1972).

Brittle deformation coefficient	Rockburst intensity
$K_u \leq 2$	No rockburst
$2 < K_u \leq 6$	Light rockburst
$6 < K_u \leq 9$	Medium rockburst
$K_u > 9$	Strong rockburst

Tang and Wang introduced another definition of rock brittleness as follows (Tang & Wang, 2002):

$$K = \frac{\sigma_c \varepsilon_f}{\sigma_t \varepsilon_b}, \quad (4)$$

where σ_c is the compressive strength of the rock, σ_t is the tensile strength of rock, $\varepsilon_f$is the strain before the peak, and ε_b is the strain after the peak. Table 8 shows the intensity of rockburst as a function of the rock brittleness index.

Table 8 Rockburst intensity based on the rock brittleness index (Tang & Wang, 2002).

Rock brittleness index	Risk of violent rupture
No rockburst	$K \leq 20$
Light rockburst	$20 < K \leq 75$
Medium rockburst	$75 < K \leq 130$
Strong rockburst	$K > 130$

4.1.2 Mean Stress (Tao Discriminant Index) (α)

This index is based on the stress reduction factor in *Q* system (Barton's classification) and defined as the ratio of UCS of rock to the maximum principal in situ stress (Grimstad, 1999; Tao, 1988) as follows:

$$\alpha = \frac{\sigma_c}{\sigma_1}, \quad (5)$$

where σ_c is uniaxial compressive strength of the rock and $\sigma_1$is maximum in situ stress. Table 9 presents the rockburst classification based on the mean stress index.

Table 9 Rockburst intensity based on the Tao discriminant index (Tao, 1988).

Mean Stress	Risk of violent rupture
No rockburst	$\alpha > 14.5$
Weak rockburst	$5.5 < \alpha \leq 14.5$
Moderate rockburst	$2.5 < \alpha \leq 5.5$
Strong rockburst	$\alpha \leq 2.5$

Hou and Wang (1989) introduced another classification or rockburst based on Eq. (5), as shown in Table 10.

Table 10 Rockburst intensity classification (Hou & Wang, 1989).

Mean stress	Risk of violent rupture
No rockburst	$\alpha \leq 0.30$
Weak rockburst	$0.30 < \alpha \leq 0.37$
Moderate rockburst	$0.37 < \alpha \leq 0.62$
Strong rockburst	$\alpha > 0.62$

Grimstad (1999) introduced another rockburst classification based on the mean stress as shown in Table 11.

Table 11. Rockburst intensity classification (Grimstad, 1999).

Mean stress	Risk of violent rupture
No rockburst	α >5
Weak rockburst	3 < α ⩽5
Moderate rockburst	2 < α ⩽3
Strong rockburst	α < 2

4.1.3 Strength Index

Hawkes (1966) defined for the first time the strength index as one of the empirical methods of rockburst prediction. The rock mass strength index (RS_i) is defined as:

$$RS_i = \frac{3\sigma_1}{\sigma_c}, \quad (6)$$

where σ_1 is the magnitude of maximum principal stress, and σ_c is UCS of rock. Table 12 shows the intensity of the rockburst based on the strength index.

Table 12 Rockburst intensity based on the strength index (Hawkes, 1966).

Strength index	Risk of violent rupture
RS_i < 0.2	Low rockburst
0.2 < RS_i ⩽ 0.4	Significant rockburst
0.4 < RS_i ≤ 0.6	High rockburst
0.6 < RS_i ≤ 0.8	Very high rockburst
0.8 < RS_i ≤ 1.0	Dangerously high rockburst
RS_i > 1.0	Unstable

4.1.4 Stress Index

The stress index (S_i) is defined as the ratio of the UCS of the rock to the vertical component of in situ stress (Yoon, 1994), which is written as

$$S_i = \frac{\sigma_c}{\sigma_v}. \quad (7)$$

Table 13 shows the intensity of rockburst based on the stress index.

Table 13 Value of stress index for prediction of rockburst (Yoon, 1994).

Stress index	Risk of violent rupture
$S_i \leq 2.5$	Heavy rockburst
$2.5 < S_i \leq 5$	Mild rockburst

4.1.5 Tangential Stress

The Tangential stress criteria are defined as the ratio of tangential stress around the excavation opening to UCS of rock (Wang et al., 1998; Hoek & Brown, 1980) as follows:

$$T_s = \frac{\sigma_\theta}{\sigma_c}. \quad (8)$$

Table 14 presents the rockburst intensity based on the tangential stress.

Table 14 Tangential stress criterion (Wang et al., 1998).

Tangential stress	Risk of violent rupture
$T_s < 0.3$	No rockburst
$0.3 \leq T_s < 0.5$	Weak rockburst
$0.5 \leq T_s < 0.7$	Strong rockburst
$T_s \geq 0.7$	Violent rockburst

Russenes (1974) introduced another empirical method to evaluate the risk of rockburst. This criterion is based on the relation of tangential stress and the strength of the rock. The method is defined as the ratio of the maximum tangential stress surrounding the rock to the UCS of rock. Table 15 shows the rockburst intensity based on the Russenes criterion.

Table 15 Rockburst prediction value based on Russenes method (Russenes, 1974).

Russenes Method	Risk of violent rupture
$\frac{\sigma_\theta}{\sigma_c} < 0.2$	No rockburst
$0.2 \leq \frac{\sigma_\theta}{\sigma_c} < 0.30$	Light rockburst
$0.3 \leq \frac{\sigma_\theta}{\sigma_c} < 0.55$	Medium rockburst
$\frac{\sigma_\theta}{\sigma_c} \geq 0.55$	Violent rockburst

4.1.6 Turchaninov Method

Turchaninov et al. (1972), defined the Turchaninov criterion to measure the rockburst intensity. This criterion is defined as

$$S = \frac{\sigma_\theta + \sigma_1}{\sigma_c}. \quad (9)$$

Table 16 represents the rockburst intensity based on the Turchaninov criterion.

Table 16 Rockburst prediction values based on the Turchaninov scholar (Turchaninov et al., 1972).

Turchaninov method	Risk of violent rupture
$S < 0.3$	No rockburst
$0.3 \leq S < 0.5$	Rockburst probably
$0.5 \leq S < 0.8$	Rockburst surely
$S \geq 0.8$	Violent rockburst

4.1.7 Failure Duration Index (D_t)

Wu and Zhang (1997) defined the failure duration index during the coal specimen. This index is expressed as the time taken for a coal specimen to break down from the peak strength to the complete failure while compressed uniaxially. Table 17 shows the rockburst tendency based on the failure duration index.

Table 17. Rockburst intensity based on the failure duration index (Wu & Zhang, 1997)

Failure duration index	Risk of violent rupture, D_t (ms)
None rockburst	D_t is larger than 500

Medium rockburst	D_t is between 500 and 50
Strong rockburst	D_t is lower than 50

4.1.8 Grimstad and Barton Classification

Grimstad and Barton (1993) introduced a criterion for rockburst prediction. They gathered data from measurement of the in situ stresses and strength of samples and could find some relationship that confirms the equations of Russenes (1974) and Hoek and Brown (1980). This criterion is defined as the ratio of UCS of rock to the maximum principal stress and the ratio of the maximum tangential stress to the UCS of rock. Table 18 shows the rockburst intensity based on the Grimstad and Barton classification.

Table 18 Rockburst intensity classification based on the Grimstad and Barton method (Grimstad & Barton, 1993).

Stress class	Description of potential induced stress	$\frac{\sigma_c}{\sigma_1}$	$\frac{\sigma_\theta}{\sigma_c}$
1	Low stress, near surface, open joints	>200	<0.01
2	Medium stress, favorable stress conditions	200–10	0.01–0.3
3	High stress, very tight structure, usually beneficial to blasting except for wall	10–5	0.3–0.4
4	Moderate spalling after > 1 h	5–3	0.5–0.65
5	Spalling and rockburst after a few minutes	3–2	0.65–1
6	Heavy rockburst and immediate strain failure	<2	>1

4.1.9 Five Factors

Zhang and Fu (2008) proposed a five-factor criterion as a compressive criterion for the prediction of rockburst. This criterion considers five involved parameters of rockburst shown in Table 19.

Table 19 Five factors (Zhang & Fu, 2008).

	No rockburst	Light rockburst	Medium rockburst	Strong rockburst
$\frac{\sigma_c}{\sigma_1}$	≤0.15	0.15–0.2	0.2–0.4	>0.4
$\frac{\sigma_\theta}{\sigma_c}$	≤0.2	0.2–0.3	0.3–0.55	>0.55
$\frac{\sigma_c}{\sigma_t}$	<15	15–18	18–22	>22

W_{et}	<2	2–3.5	3.5–5	>5
K_u	≤0.55	0.55–0.60	0.60–0.80	>0.80

Note: σ_1 is the maximum in situ stress, σ_θ is tangential stress, σ_c is UCS of rock, σ_t is the tensile strength of tock, W_{et} is elastic strain energy, and K_u is brittle deformation coefficient.

4.1.10 Hoek and Brown Classification

The rock mass strength is normally assessed by back analyzing case histories where examples of failure have been precisely documented (Sakurai, 1993). Rock mass failure around excavation opening occurs in a form of spalling or fracturing, and back analyses can estimate the induced stresses required to cause this fracturing. Hoek and Brown (1980) proposed a complete description of brittle failure with the same criterion that can determine the rock mass instability around the excavation opening. This criterion is defined as the ratio of maximum far field stress to the UCS of rock. Table 20 shows the intensity of rockburst based on the Hoek and Brown classification.

Table 20. Rockburst intensity based on the Hoek and Brown classification (Hoek & Brown, 1980)

H-B criterion	Risk of violent rupture
$\frac{\sigma_c}{\sigma_1} \leq 0.1$	No damage
$\frac{\sigma_c}{\sigma_1} = 0.2$	Minor spalling
$\frac{\sigma_c}{\sigma_1} = 0.3$	Severe spalling
$\frac{\sigma_c}{\sigma_1} = 0.4$	Very severe spalling
$\frac{\sigma_c}{\sigma_1} = 0.5$	Stability of opening may be very difficult to achieve

However, this criterion cannot be applied to the other stress conditions or mining situations because it is based on experiences of 3 or 4 m^2 of tunnels in brittle rocks in South Africa's gold mines according to the database of Ortholep and his colleagues (Ortlepp & Stacey, 1994).

4.1.11 Rock Mass Index (RMi)

The rock mass index was introduced as a rock mass characterization system for rock engineering purposes (Palmstrom, 1995) .The main objective of the RMi is to improve the geological input data. The RMi equation is written as

$$\text{RMi} = \sigma_c \times J_p , \tag{10}$$

where σ_c stands for the UCS of rock, and J_p is the jointing parameter composed of the block volume and roughness, and alteration and size characteristics of joints. Based on the studies of Palmstrom (1995), the *RMi* of massive rocks is defined as follows:

$$\mathrm{RMi} = f_{\mathrm{a}} \times \sigma_{\mathrm{c}}\,, \tag{11}$$

where f_{a} is the factor related to the scale effect of compressive strength and the range is between 0.45 and 0.55. Therefore, the competency factor can be defined as

$$C_{\mathrm{g}} = \frac{\mathrm{RMi}}{\sigma_{\theta}} = f_{\mathrm{a}} \times \frac{\sigma_{\mathrm{c}}}{\sigma_{\theta}}\,. \tag{12}$$

Table 21 shows the rockburst intensity based on the value of the competency factor.

Table 21 Rockburst intensity based on the RMi (Palmstrom, 1995).

Competency factor , C_{g}	Failure mode
> 2.5	No rock stress-induced instability
2.5 – 1	High stress, slightly loosening
1 – 0.5	Light rockburst or spalling
< 0.5	Heavy rockburst

4.2 Energy Methods

The magnitude of stored strain energy within the rock mass is changed during the excavation process. Therefore, one of the effective indicators for rockburst prediction could be the release of stored strain energy of rock during the underground excavation process. Hence, rock mass-energy analysis can be used to explain the type and intensity of rockburst. In this regard, Cook (1963) conducted one of the earliest studies to show energy changes in the rock mass in underground mining when the excavation was taken place. Afterward, the researcher studied the relationship between the energy changes of rock mass and rockburst mechanism, generating an acceptable theory of elasticity for the simulation of the rock mass behavior around the excavation area. In the next section, the important rockburst prediction methods, based on the rock stored energy, will be reviewed.

4.2.1 Elastic Strain Energy Index

The stored elastic energy in the rock is considered a significant way to calculate the intensity of rockburst. Kidybiński defined the elastic strain energy index as a complete stress–strain curve, as follows (Kidybiński, 1981):

$$R = \frac{W_{\mathrm{E}}}{W_{\mathrm{P}}}\,, \tag{13}$$

where W_{E} is the elastic strain energy saved before the rock failure, and W_{P} is the plastic strain energy consumed after rock failure. Figure 8 depicts the complete stress–strain curve. Based on the elastic strain energy index, rockburst intensity is categorized in Table 22.

Table 22 Energy index value (Kidybiński, 1981).

Elastic strain energy	Risk of violent rupture
$R < 2$	No rockburst
$2 \leq R < 5$	Slightly rockburst
$R \geq 5$	Severely rockburst

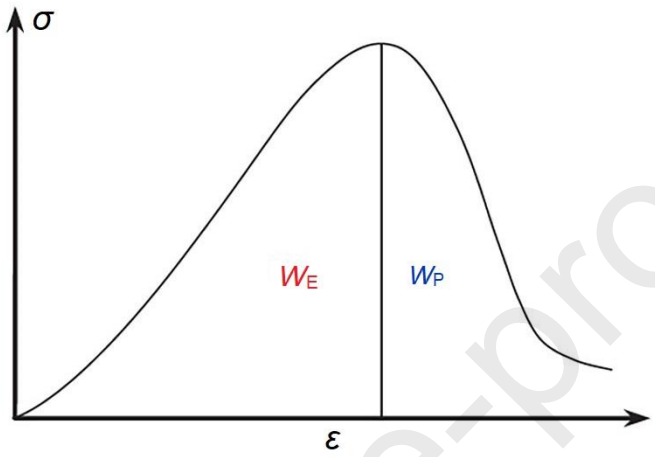

Fig. 8. The complete stress–strain curve (Kidybiński, 1981).

4.2.2 Liner Elastic Energy and Burst Potential Index (BPI)

Wang and Park (2001) firstly introduce the linear elastic energy (W_{et}), which is defined as the linear elastic energy stored in the rock specimen before the rock failure point, expressed as

$$W_{\mathrm{et}} = \frac{\sigma_c^2}{2E_{\mathrm{u}}}, \tag{14}$$

where σ_c is the UCS of intact rock (MPa), and E_u is the elastic modulus. Table 23 shows the rockburst intensity based on the value of linear elastic energy.

Table 23 Rockburst intensity based on the linear elastic energy (Wang & Park, 2001).

Liner elastic energy	Risk of violent rupture
Weak rockburst	$W_{et} < 50$ kJ/m^3
Moderate rockburst	50 Kj/m^3 < W_{et} < 100 kJ/m^3
Strong rockburst	100 Kj/m^3 < W_{et} < 200 kJ/m^3
Extra strong rockburst	$W_{et} > 200$ kJ/m^3

The linear elastic energy has a relationship with the brittleness coefficient (Lee et al., 2004), as follows:

$$W_{\mathrm{et}} = 213.94 \ln(B_{\mathrm{i}}) - 321.10 \ , \tag{15}$$

where B_{i} is the brittleness coefficient.

Singh (1988) also introduced BPI, which is defined as the ratio of the strain energy retained, E_{R}, to the permanent strain energy, E_{D}. The BPI is written in Eq. (16) as follows:

$$\mathrm{BPI} = \frac{E_{\mathrm{R}}}{E_{\mathrm{D}}} . \tag{16}$$

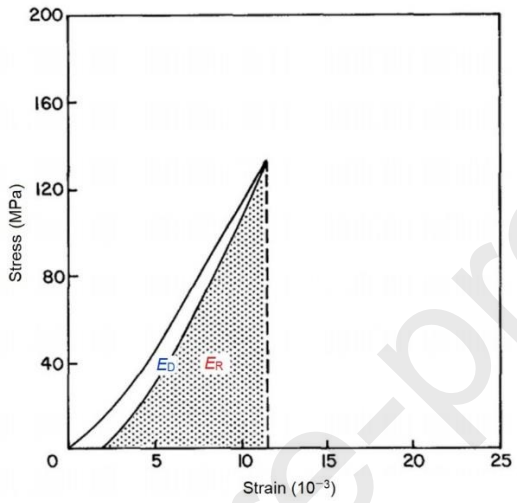

Fig. 9. Typical stress–strain curve for loading and unloading during uniaxial compression test (Singh, 1988).

Despite the advantage of BPI criterion, achieving 80% – 90% of the rock strength with BPI is a problem because of two reasons: first, the strength can be known only in a probabilistic manner; second, the value of the index is influenced by the relative value of the load attained. Therefore, another index, called Brittleness Index Modified (BIM), was proposed to eliminate this problem (Gill et al., 1988). The BIM equation is written in Eq. (17) as follows:

$$\mathrm{BIM} = \frac{A_2}{A_1} , \tag{17}$$

where A_2 represents the area under the loading curve, and A_1 is the area under the line corresponding to the elastic modulus of the rock (E) (Fig. 10). When the BIM increases, additional energy is dissipating during loading, and less energy is available for violent rupture. Aubertin et al. (1994) proposed a risk classification for rockburst based on the value of the BIM, as shown in Table 24.

Table 24 BIM indicative values and risk of violent rupture (Aubertin et al., 1994).

BIM	Risk of violent rupture
Between 1.00 and 1.20	High
Between 1.20 and 1.50	Moderate
More than 1.50	Low

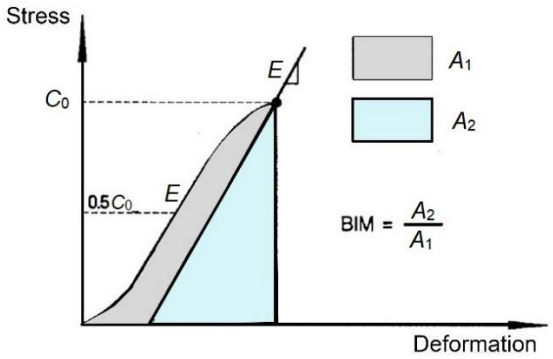

Fig.10. Determination of BIM with uniaxial compression tests (Aubertin et al., 1994).

Regarding the results from the comparison of the empirical and simulation methods, a new rockburst prediction index was introduced (Jiang et al., 2010), called the rockburst energy release rate (RBERR) as follows:

$$\mathrm{RBERR} = \frac{\mathrm{LERR}}{\mathrm{LESR}} = \frac{U_{i\max} - U_{i\min}}{\mathrm{LESR}} = \frac{U_{i\max} - U_{i\min}}{\mathrm{LESR}}, \tag{18}$$

where LERR is the local energy release rate (LERR), and LESR is the limit energy storage rate. LERR is defined as the sudden energy release of the element; $U_{i\max}$ and $U_{i\min}$ are the peak values of elastic strain energy intensity before and after the brittle failure of the *i*th element, respectively, expressed as

$$\begin{cases} U_{i\max} = \frac{[\sigma_1^2+\sigma_2^2+\sigma_3^2-2\nu(\sigma_1\sigma_2+\sigma_2\sigma_3+\sigma_1\sigma_3)]}{2E} \\ U_{i\min} = \frac{\left[\sigma'^2_1+\sigma'^2_2+\sigma'^2_3-2\nu(\sigma'_1\sigma'_2+\sigma'_2\sigma'_3+\sigma'_1\sigma'_3)\right]}{2E} \end{cases}, \tag{19}$$

where σ_1, σ_2, and σ_3 are the three principal stresses corresponding to the peak strain energy of the element; σ_1', σ_2', and σ_3' are three principal stresses corresponding to the minimum strain energy of the element; ν is the Poisson's ratio; E is Young's modulus. LERR reflects the different conditions after excavation, for example, the limited energy storage capacity of the rock mass and the different stress status in a rock mass.

4.2.3 Rock Mass Integrity Coefficient

This criterion is used to evaluate the rockburst intensity and defined as the ratio of rock mass elastic wave speed to the rock elastic wave (Yoon, 1994) as follows:

$$K_{\mathrm{V}} = \frac{V_{\mathrm{pm}}^2}{V_{\mathrm{pr}}^2}. \tag{20}$$

Table 25 shows the rockburst tendency based on the rock integrity coefficient.

Table 25 Rockburst prediction tendency based on the rock integrity coefficient (Yoon, 1994).

Rock integrity coefficient	Risk of violent rupture

$K_V < 0.5$	No rockburst
$0.5 \leq K_V < 0.6$	Weak rockburst
$0.6 \leq K_V < 0.75$	Medium rockburst
$0.75 \leq K_V < 1.0$	Strong rockburst

4.2.4 Seismic Energy

Spottiswoode and McGarr (1975) proposed for the first time the radiated energy of rockburst, monitored by a microseismic technique. In this regard, the relationship between rockburst radiated energy and intensity of rockburst was studied. Based on the results, the radiated energy was considered as an evaluation index for the rockburst intensity classification. Table 26 shows the new classification based on the common logarithms of radiant energy.

Table 26 Rockburst classification based on the logarithm of radiant energy (Spottiswoode & McGarr, 1975) .

Seismic method	Risk of violent rupture
No rockburst	$\lg(E/J) < 2$
Weak rockburst	$0 \leq \lg(E/J) < 2$
Moderate rockburst	$2 \leq \lg(E/J) < 4$
Intense rockburst	$4 \leq \lg(E/J) < 7$
Extremely intense rockburst	$\lg(E/J) \geq 7$

Note: $\lg(E/J)$ is the average common logarithm of the rockburst radiated energy. This radiated energy is recorded by microseismic station at the location of mining. E/J is called energy per joule and it is the unit of rockburst radiated energy.

Then, Chen et al. (2013) studied seismic energy at Jinping II Hydropower Station in China to find a new index for the seismic energy. They investigated the characteristics, magnitude, laws of the radiated energy, and the relationship between the rockburst radiated energy and intensity. From the research results, a new set of criteria for the quantitative classification of the rockburst intensity was introduced based on radiated energy and rock damage severity, as shown in Table 27.

Table 27 Rockburst intensity quantitative classification criteria based on radiated energy with rock mass failure intensity (Chen et al., 2013)**.**

Rockburst levels	lg (E/J)	Main phenomena

None	$(-\infty, 0]$	The crack occurred inside rock mass; an evident failure cannot be found on the surface of the rock mass, and the cracking sound could barely be heard; no support system and construction are affected
Weak	(0, 2]	Main failure type was slight spalling and slabbing in the surface surrounding rock mass; the rock mass was slightly ejected; the size of the ejected fragment was 10–30 cm; the cracking could be heard slightly, and the depth of failure was <0.5 m
Moderate	(2, 4]	The main failure type was severe spalling and slabbing of the surrounding rock mass; the rock mass was evidently ejected; the size of the ejected fragment was 30–80 cm; the cracking was similar to a diameter blasting and lasted for some time inside the rock mass
Intense	(4, 7]	A great deal of rock mass was suddenly ejected; the failure range was extensive; the size of ejected fragment was 80–150 cm; the edge of the failure zone typically has a fresh fracture plane; the rockburst is similar to an explosive
Extremely intense	$(7, \infty]$	A large block of rock mass was suddenly ejected with intensive seismically, and the stability was seriously damaged; the depth of the failure was more than 3 m

4.2.5 Excess Shear Stress (ESS)

Ryder firstly proposed the ESS criterion, which is based on available energy when passing from static resistance (before slip movement) to the dynamic resistance (during slip) (Ryder, 1987). The static resistance of discontinuities (T_s) can be calculated using the Mohr-Coulomb criterion as follows:

$$\tau_s = c + \mu_s \sigma_n \,, \tag{21}$$

where c is the static cohesion, σ_n is the normal stress, and μ_s is the static friction angle. Therefore, the value of ESS is obtained from the following equation (Eq. (22)):

$$\text{ESS} = \tau_s = |\tau| - \tau_d \,, \tag{22}$$

where τ_s is the net shear stress available to produce a seismic event, τ is the shear stress at the initiation point, and τ_d is dynamic resistance at this point which is given by Eq. (23):

$$\tau_d = \mu\, \sigma_n \,. \tag{23}$$

If ESS value brought by the progression of the excavation toward the discontinuity is large, then the surface of the discontinuity involved would also be large, and the seismic event would produce a large surface. However, the back analysis showed that not all positive ESS situation yielded seismic events, which may be due to the lack of accuracy of data or stress involved. Gill et al. (1994) and Ryder, (1987) noted that this lack of rockburst for positive ESS confirms the discontinuity post-peak stiffness. If the post-peak stiffness of the rock specimen is less than the load system stiffness, then the equilibrium state becomes unstable, and the failure of the rock specimen is violent. Otherwise, the equilibrium state becomes stable and the failure occurs

gradually. In addition, the rock mass stiffness on both sides of the discontinuity may play a major role in this process.

4.2.6 Fractional Energy Release Rate (FERR)

Based on the energy release rate (ERR) and the LERR, Xiao, et al. (2016) introduced a new index as a frictional energy release rate (FERR). The ERR is an important index to evaluate the stability of the rock which has been confirmed by many researchers. The ERR can evaluate the rockburst intensity. However, the location, intensity, and scale of rockburst are not clear when the ERR is applied. Moreover, ERR is an average ERR of tunnel excavation, and when the tunnel excavation processes, the average of ERR is not suitable to estimate the local energy released. The LERR is an index to describe the energy released from a certain element in each excavation step. However, this index is based on the elastic assumption. Therefore, the failure of rock cannot be considered. The new index (FEER) was proposed to overcome the disadvantages of ERR and LERR. The FERR can be defined as follows (Eqs. (24)–(27)):

$$\mathrm{FERR}_i = \frac{E_i}{V_i}, \tag{24}$$

$$\mathrm{FV}_i = V_i, \tag{25}$$

where E_i and V_i are calculated by Eqs. (26) and (27), respectively:

$$E_i = \sum_{j=1}^{m} \mathrm{LERR}_j . V_j, \tag{26}$$

$$V_i = \sum_{j=1}^{m} V_j, \tag{27}$$

where E_i is the total released energy of failed rock in interval *i*, LERR_j is the local released energy of broken element *j*, V_j is the volume of broken element *j*, V_i is the total volume of broken elements in statistic interval *i*, and *m* is the total broken elements of statistic interval *i*.

4.2.7 Burst Efficiency Ratio

Singh (1989) proposed the burst efficiency ratio as follows (Eq. 28):

$$\eta = \left(\frac{E_\mathrm{t}}{E_\mathrm{s}}\right) \times 100, \tag{28}$$

where E_t is the energy of rock fragments after the failures of a specimen under uniaxial compressive stress, and E_s is the maximum elastic strain energy. Table 28 shows the burst efficiency ratio based on the rockburst intensity.

Table 28 Rockburst intensity based on the burst efficiency ratio (Singh, 1989).

Rock of violence rupture	Burst efficiency
No rockburst	η < 3.5%
Light rockburst	3.5% ≤ η < 4.2%
Medium rockburst	4.2% ≤ η < 4.7%

Strong rockburst	$\eta \geq 4.7\%$

4.3 Other Rockburst Prediction Methods

Despite the stress and energy methods of rockburst prediction, some rockburst prediction criteria that are less common than stress and energy methods exist. Goel (1994) developed an empirical method based on the rock mass number *N*, defined as *Q* with SRF = 1. The rock mass number is defined by the equation :

$$N = \left[\frac{\mathrm{RQD}}{J_\mathrm{n}}\right]\left[\frac{J_\mathrm{r}}{J_\mathrm{a}}\right][J_\mathrm{w}]\,, \tag{29}$$

where RQD is the rock quality designation, J_n is the number of joint sets, J_r is the roughness of the most unfavourable joint or discontinuity, J_a is the degree of alteration or filling along the weakest joint and J_w is the joint water parameter. Eq. (29) represents that N is Barton's rock mass quality with SRF 1. *N* is used to avoid the problems and uncertainties in obtaining the correct rating of parameter SRF in *Q* method. By considering the tunnel depth (*H*), the tunnel span or diameter (*B*) and the rock mass number (*N*), the log-log plot between *N* and $HB^{0.1}$ was made by Goel and Jethwa (1995). The data points above the red line represent squeezing conditions, whereas the points below show non-squeezing conditions (Fig. 11). The equation of line *AB* separates the squeezing and non-squeezing cases (Its equation is $H = (275N^{0.33})B^{-0.1}$). As can be seen from Table 29, these demarcation lines are defined mathematically. These equations can be used to estimate the ground conditions and fix to the tunnel alignment through a better rock mass or reduced thunnel depth to avoid squeezing conditions and related tunneling problems.

Table 29 Prediction of ground conditions for tunneling (Goel & Jethwa, 1995) (u_a is the tunnel closure/deformation, a is the tunnel radius in m, u_a/a is the normalised tunnel convergence in %, *N* is the stress free *Q*, J_r is the Barton's joint toughness number and J_a is the Barton's joint alternation number)

Number	Ground conditions	Equations for predicting ground conditions
1	Self-supporting	$H < (23.4\ \mathrm{N}^{0.88})B^{-0.1}$ & $B < 2Q^{0.4}$
2	Non-squeezing	$(23.4\ N^{0.88})B^{-0.1} < H < (275\ N^{0.33})B^{-0.1}$
3	Minor squeezing ($\frac{u_\mathrm{a}}{a} < 1\%$)	$(275\ N^{0.33})B^{-0.1} < H < (450\ N^{0.33})B^{-0.1}$ $\frac{J_\mathrm{r}}{J_\mathrm{a}} < 0.5$
4	Severe squeezing ($\frac{u_\mathrm{a}}{a} < 3\%$ to 5%)	$(450\ N^{0.33})B^{-0.1} < H < (630\ N^{0.33})B^{-0.1}$ $\frac{J_\mathrm{r}}{J_\mathrm{a}} < 0.5$
5	Very severe squeezing $\frac{u_\mathrm{a}}{a} > 5\%$	$H > (630\ N^{0.33})B^{-0.1}$ $\frac{J_\mathrm{r}}{J_\mathrm{a}} < 0.25$

According to parameters in Table 29, the size of a tunnel will affect the ground condition. This is probably because as the tunnel diameter increases, the rock mass confinement decreases and therefore the rock mass strength decreases. Also, when the ratio of J_r/J_a is more than 0.5, the probability of rockburst increases as well, as shown in Fig. 11. By looking at this graph and its equations, we can calculate the ground conditions for tunneling, the types of squeezing conditions, and the rockburst.

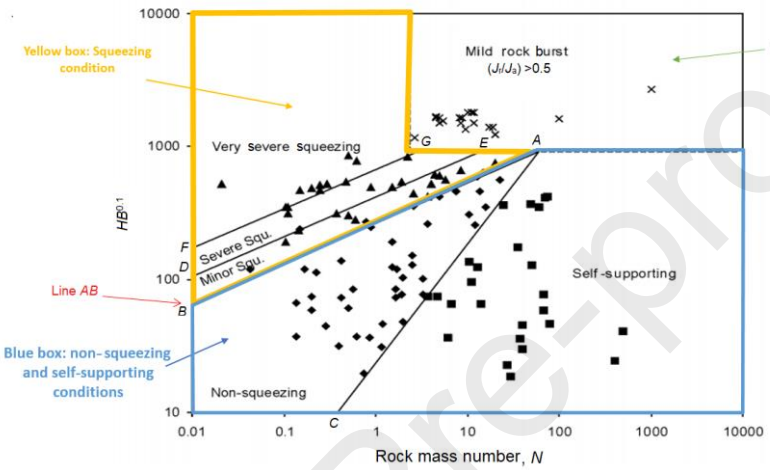

Fig. 11. Prediction of squeezing ground condition (Goel, 1994).

Singh et al. (1997) also proposed a criterion for rockburst prediction as ground condition evaluation. This criterion is defined as a function of the rock mass quality index, the overburden thickness, and the opening width. Zhao et al. (2017) modified and proposed a new value for the rockburst intensity. The database of Qirehataer Diversion tunnel excavation in Gneissic Granite was used in this study. The location of the tunnel was 15.66 km long with a depth of 1720 m under the ground surface. Three rockburst prediction methods were used to evaluate rockburst intensity, namely, Barton, Russene, and Hoek and Brown methods (Hoek & Brown, 1980; Barton, et al., 1974; Russenes, 1974). Table 30 shows the results of the modified rockburst classification. The modified method is based on the revised ratio of principal stress over strength. Moreover, two prediction methods, original and modified methods, were compared with each other. The results showed that when the modified prediction methods were employed, the data interpretation had given better results than that of the original prediction method. The modified method could enhance the consistency of these three criteria.

Table 30 Original and modified criterion (Zhao et al., 2017).

Prediction method	Details of criterion	No rockburst	Light rockburst	Moderate rockburst	Strong rockburst	Very strong rockburst
Barton	Original prediction classification	$\frac{\sigma_c}{\sigma_1} > 5$	$2.5 < \frac{\sigma_c}{\sigma_1} < 5$		$\frac{\sigma_c}{\sigma_1} \leq 2.5$	
	Modified criterion classification	$\frac{\sigma_c}{\sigma_1} > 5$	$4 < \frac{\sigma_c}{\sigma_1} \leq 5$	$2.5 < \frac{\sigma_c}{\sigma_1} \leq 4$	$1.5 < \frac{\sigma_c}{\sigma_1} \leq 2.5$	$\frac{\sigma_c}{\sigma_1} \leq 1.5$
Russenes	Original criterion classification	$\frac{\sigma_\theta}{\sigma_c} < 0.2$	$0.2 \leq \frac{\sigma_\theta}{\sigma_c} < 0.3$	$0.3 \leq \frac{\sigma_\theta}{\sigma_c} < 0.55$	$\frac{\sigma_\theta}{\sigma_c} > 0.55$	
	Modified criterion classification	$\frac{\sigma_\theta}{\sigma_c} \leq 0.2$	$0.2 < \frac{\sigma_\theta}{\sigma_c} \leq 0.5$	$0.5 < \frac{\sigma_\theta}{\sigma_c} \leq 0.7$	$0.7 < \frac{\sigma_\theta}{\sigma_c} \leq 0.9$	$\frac{\sigma_\theta}{\sigma_c} > 0.9$
Hoek and Brown	Original prediction classification	$\frac{\sigma_c}{\sigma_v} > 7$	$\frac{\sigma_c}{\sigma_v} = 3.5$	$\frac{\sigma_c}{\sigma_v} = 2$	$\frac{\sigma_c}{\sigma_v} = 1.7$	$\frac{\sigma_c}{\sigma_v} = 0.5$
	Modified criterion classification	$\frac{\sigma_c}{\sigma_v} > 10$	$5 < \frac{\sigma_c}{\sigma_v} \leq 10$	$3.3 < \frac{\sigma_c}{\sigma_v} \leq 5$	$2.5 < \frac{\sigma_c}{\sigma_v} < 3.3$	$\frac{\sigma_c}{\sigma_v} \leq 2.5$

The other method of rockburst prediction is Rock Quality Designation (RQD) index of the rock mass, which shows the degree of rock mass integrity. RQD is a simple but useful index for rockburst prediction, developed by Tang (2000) . According to the RQD classification system, the probability of rockburst increases with increasing the RQD index (Wang & Park, 2001; Xu, et al., 2008; Zhou, et al., 2012). Xu et al. (2008) found that the probability of rockburst is likely to occur when the RQD is more than 60% . Table 31 shows the classification of rock mass based on the RQD index.

Table 31. RQD classification (Tang, 2000).

RQD	Risk of violent rupture
<25%	No
25%–50%	Light
50%–75%	Medium

75%–90%	Strong
90%–100%	Very strong

Based on the 3D stress field analysis, Tajduś proposed several rockburst criteria for the evaluation of rockburst potential, including the energetic rockburst indicator (Tajduś, et al., 1997). This method is defined as

$$T = \frac{E_{\mathrm{k}}}{E_{\mathrm{k}}^{\mathrm{o}}}, \tag{30}$$

where E_{k} is the accumulated energy in the rock mass, and $E_{\mathrm{k}}^{\mathrm{o}}$ is the required energy for initiating the rockburst. Hence, E_{k} and $E_{\mathrm{k}}^{\mathrm{o}}$ can be defined as follows:

$$E_{\mathrm{k}} = V_{\mathrm{c}} + E_{\mathrm{n}} - L_{\mathrm{zv}}, \tag{31}$$

$$E_{\mathrm{k}}^{\mathrm{o}} = \frac{1}{2}\rho_{\mathrm{v}} V_0^2, \tag{32}$$

where V_{c} is elastic energy accumulated in the broken rock mass during rockburst, E_{n} is energy generated by the tremor in the rock mass, L_{zv} is used for breaking and crushing rock mass volume discharged to an opening, ρ_{v} is the average density of broken rock mass (2.5 t/m^3), and V_0 is the average velocity of broken rock mass acting on an opening surface during rockburst (10 m/s). Therefore, the value of $E_{\mathrm{k}}^{\mathrm{o}}$ is equal to 1.25×10^5 J/m^3. Table 32 shows the rockburst intensity based on the energetic rockburst indicator.

Table 32 Rockburst occurrence based on the energetic rockburst indicator (Tajduś et al., 1997).

Energetic rockburst indicator	Risk of violent rupture
No rockburst	$T < 1$
Rockburst	$T \geq 1$

4.4 Literature Review on Stress, Energy, and numerical Methods of Rockburst Prediction

In rockburst occurrence, all geomechanical parameters of rock have a significant effect on rockburst occurrence. Aside from these factors, the magnitude of in situ stresses, the presence of water, and rock structure are related to the intensity, shape, and location of rockburst occurrence. As mentioned, empirical methods of rockburst are based on the analysis of rockburst from different perspectives, including stresses around the excavated rock, strength of rock, energy conversion during the excavation, and depth of excavation. These methods have been extensively used for different purposes, such as the determination of rockburst intensity in underground excavation and the utilization of these methods as input data on numerical and intelligent methods of rockburst prediction. Singh (1987) used the rock brittleness coefficient (Eq. (1)) to express the effect of intact rock properties on the rockburst intensity. Based on the results, brittleness, compressive and point load strengths, modulus of rigidity, and compressional wave velocity have strong influences on the

Burst Proneness Index (BPI). The rockburst can occur at a certain combination of geologic and mining conditions, and the elastic characteristic plays an important role in the hard rocks. In addition, hard, brittle, and elastic rocks have a high potential for bursting. In 1988, Singh used the elastic strain energy (Eq. (13)) index to show a parameter that represents the energy released at the time of rock fracture and to determine the important indices and rock properties as an important factor of bursting (Singh, 1988). Based on the results, decreasing the modulus index depends on the burst-proneness index, strength, brittleness, and the strain energy stored in the rock specimens. Wang and Park (2001) studied the prediction of rockburst based on the analysis of strain energy within the rock (Eq. (16)). This study focuses on the investigation of potential and tendency of rockburst during the mining at a depth of −570 m. In this regard, several empirical methods of rockburst prediction were employed as the input data of numerical modeling to determine the rockburst intensity in the Linggold gold mine in China. The results showed that numerical modeling should be employed along with the empirical methods of rockburst prediction to provide reliable results. Du et al. (2010) also used empirical methods of rockburst prediction, such as brittleness coefficient (Eq. (1)), deformation brittleness index (Eq. (2)), and elastic energy index (Eq. (13)) in Chengchao Iron Mine in China, for the simulation of rockburst tendency at the depth of −430 to −700 m. Moreover, tensile and UCS tests were conducted to determine the geomechanical parameters of rocks. The significant result of this study is that the probability of rockburst hazard and the critical depth of mine were identified as important factors in the mining design and rockburst prediction field. Zhou et al. (2012) employed different rockburst prediction methods, as input data of the support vector machines, for the determination and classification of long-term rockburst in underground excavations. A total of 132 rockburst events were compiled from various published studies, and five different models were investigated. The maximum tangential stress, UCS, tensile strength of the surrounding rock, rock brittleness coefficient (Eq. (1)), elastic strain energy index (Eq. (13)), and depth were regarded as the input data. On the contrary, the actual rockburst intensity was considered the output result. In several models, the stress coefficient (Eq. (7)) and the rock brittleness coefficient (Eq. (1)) were added to the input data. The results proposed that the developed models in this study can be used for the rockburst prediction, which may help to reduce the impacts of the rockbursts. Wang et al. (2015) studied the prediction of rockburst based on the fuzzy-matter elements and the empirical methods were used as the input data of fuzzy-matter elements. The study area was in Huized-Lead Zink mine in China. Zhou et al. (2016a) conducted another study on the intelligent rockburst prediction methods and selected several criteria of rockburst prediction as the input data for the cloud model with entropy weight . The entropy-cloud model was used to determine the weight of every input data. From the results, the stress coefficient, tangential stress, and the elastic energy index have shown to play a greater role compared with the brittleness coefficient, UCS, and tensile strength of the rock in the prediction of the rockburst. Zhou et al. (2016b) conducted a study on feasibility of stochastic gradient boosting approach for the rockburst prediction. In this study, they examined a database of 254 rockburst events using stochastic gradient boosting methods (SGB) in order to categorize rockburst damage. Five factors have been evaluated, including the stress condition factor, the ground support system capacity, excavation span, geological structure, and peak particle velocity. Multiclass problems were assessed using two accuracy measures: classification accuracy rate and Cohen's Kappa. The

accuracy analysis together with Kappa of the rockburst damage dataset shows that the SGB model is acceptable for predicting rockburst damage. Zhou et al. (2016c) investigated on classification of rockburst in underground projects and compared then supervised learning (SL) methods. A data set of 246 rockburst events was analyzed for rockburst classification using (SL) methods. Eight potentially relevant indicators were used to analyze the data set such as depth (H), rock mass intact coefficient (MTS), uniaxial compressive strength of rock, strain energy storage (W_{et}), stress concentration (SCF), rock brittleness index (B_1) and B_2 ($(\sigma_c - \sigma_t)/(\sigma_c + \sigma_t)$). They are considered among the most important quantifiable indicators of rockburst behavior. On the basis of their ability to learn rockburst, 11 algorithms from 10 categories of SL algorithms were evaluated, including linear discriminant analysis (LDA), quadratic discriminant analysis (QDA), partial least-squares discriminant analysis (PLSDA), naïve Bayes (NB), k-nearest neighbor (KNN), multilayer perceptron neural network (MLPNN), classification tree (CT), support vector machine (SVM), random forest (RF), and gradient-boosting machine (GBM). For multiclass problems, two accuracy measures were used: classification rate and Cohen's Kappa. Regarding to the results, GBM and RF were the most accurate models for rockburst prediction. Cai (2016) applied rockburst prediction criteria to determine the rockburst intensity in Sanshandao Gold Mine in China as a study case. They aim to develop a theory and technique for understanding the rockburst mechanism based on the analysis of disturbance energy. Results show that two conditions are necessary for the occurrence of rockburst in the underground excavation. The first one is that the rock mass must have a good condition to store strain energy, and the second one depends on geological stress conditions of the underground excavation area. Miao et al. (2016) studied the occurrence of rockburst in Sanshadoa Gold Mine in China as a case study, and the location and intensity of rockburst during mining activity were predicted by empirical methods of rockburst prediction and numerical simulations. Hence, the main rock at a great depth of Sanshadoa Gold Mine is prone to rockburst occurrence, and the magnitude of in situ stresses is a significant factor for rockburst prediction. Xue et al. (2019) proposed a new rockburst evaluation method based on the rough set theory and extension theory . This method was applied to the underground caverns of Jiangbian Hydropower Station in China's Sichuan Province as a case study. For this study, significant methods of rockburst prediction, such as elastic strain energy index (Eq. (13)), rock integrity (Eq. (20)), rock brittleness coefficient (Eq. (1)), mean stress (Eq. (5)), and tangential stress (Eq. (8)) were analyzed and have been taken into the rough set theory. According to the results of the rough set theory (Xue et al., 2019) , the main influential indexes and their weight were used in the extension theory to predict rockburst as a new rockburst evaluation method. Based on the results of this study, the proposed method of rockburst prediction has shown acceptable performance in real conditions. In this way, the rockburst grades and rockburst types are evaluated more comprehensively. Zhou et al. (2021) developed a hybrid system containing the firefly algorithm (FA) and an artificial neural network (ANN) to predict and classify rockburst in underground geotechnical engineering projects. A total of 196 reliable rockburst cases regarding this phenomenon were collected from deep mines and tunnels. As a result of the new hybridized model FA–ANN, the accuracy of rockburst prediction was significantly enhanced. Ahmed et al. (2017) studied the rockburst occurrence in the shaft station area of the Provence Coal Mine in South France. The mined coal had a 2.5 m thickness and a 10° dip angle. The area of the shaft station was

at 1000 m depth. This study aimed to investigate the rockburst occurrence where the pillars and longwall panels excavated. Empirical methods of rockburst, such as BPI (Eq. (16)), rock brittleness coefficient (Eq. (1)), and mean stress (Eq. (5)) were applied to estimate rockburst tendency. Moreover, a simulation model comprising an excavation area (a large-scale finite difference numerical model regarding the area of the shaft with its irregular pillars) was employed. The results showed that vertical stress increased in the shaft station pillars due to excavation of long wall panels, and hence, the small pillars are more prone to the rockburst than the large ones. Moreover, the BPI method can be used to evaluate the risk of rockburst in pillars. Xu et al. (2018) studied new rockburst prediction and classification methods in underground excavation. The new model was established by introducing the basic theory of ideal point methods, regarding the rockburst mechanism. The ideal-point method is an analytical method for multi-objective decision-making and can transform a multi-objective programming problem into a single-objective one. For the evaluation of rockburst in this model, the rock stress coefficient (Eq. (7)), rock brittleness coefficient (Eq. (1)), and elastic strain energy (Eq. (13)) were selected as significant empirical methods of rockburst prediction. A principal component analysis based on mutual information (MIPCA) for the rockburst feature selection was used to calculate a new group of parameters to eliminate any correlation between the parameters. MIPCA was used to consider weight on the selected parameters, and finally, a computer-prediction grading system for rockbursts was developed based on the proposed ideal-point model. This computer system works with measured project data, including maximum tangential stress, the UCS, and elastic energy index and shows an acceptable accuracy for rockburst prediction. Zhou et al. (2020) developed a neuro-bee intelligent system for prediction of rockburst. A hybrid technique of the artificial neural network (ANN) and artificial bee colony (ABC), namely, the neuro-bee model, was used in this study to create a sophisticated relationship between the risk of rockbursts in burst-prone grounds and its influencing factors. The indicators were the maximum tangential stress of the cavern wall (σ_θ), the uniaxial compressive strength (UCS) of rock, the uniaxial tensile strength of rock, the stress concentration factor (SCF) and the rock brittleness index. Based on the results, the new hybrid model provides more accurate rockburst predictions in both prediction accuracy and generalization capability when compared to other prediction methods. Ma et al. (2018) studied a novel rockburst prediction criterion based on the TBM tunnel construction of the Neelum–Jhelum (NJ) hydroelectric project in Pakistan. Empirical methods were selected to determine the new rockburst criterion (Eq. (1) and Hoek and Brown criterion, Section 4.1.10). Moreover, geomechanical parameters of rock were evaluated by considering rock strength, brittleness coefficient, quantitative GSI, the TBM construction disturbance, and the in situ stress state. The newly proposed method was defined as the ratio of rock mass strength based on the Hoek-Brown strength criterion to the maximum horizontal stress perpendicular to the tunnel axis. Based on the results, this method could enhance the accuracy of rockburst during the excavation of underground mining. Pu et al. (2018) presented a method for rockburst prediction where no enough data for rockburst prediction exist. For this purpose, the decision tree was utilized as an intelligent method for rockburst prediction. The two Kimberlite pipes at the Diamond Mine in North Canada were selected as case study. For evaluation of rockburst, several empirical methods of rockburst prediction, such as linear elastic energy (Eq. (14)), rock brittleness coefficient (Eq. (1)), the ratio between maximum shear stress around the

tunnel wall, and uniaxial tensile stress were used. The decision tree model was built for 108 samples where the rockburst occurred and its accuracy was 73% when empirical methods of rockburst were employed. By contrast, this model showed an accuracy of 93% for 132 incomplete data sample. Lee et al. (2004) focused on a new scale system of brittleness and UCS to evaluate the rockburst intensity. Hence, a relationship between the rock brittleness coefficient and UCS of intact rock was obtained:

$$\mathrm{UCS} = 110.45 \ln (B_{\mathrm{i}}) - 114.84 , \quad (33)$$

where B_{i} is the rock brittleness coefficient. The other relationship between UCS and SED was obtained as follows:

$$\mathrm{UCS} = 10.25\ \mathrm{SED}^{0.25} . \quad (34)$$

Moreover, SED, rock brittleness coefficient, and UCS have a significant relationship with rockburst occurrence. According to their results, the value of each rockburst class was suggested based on the three significant factors. Table 33 shows the rockburst intensity based on these rockburst prediction factors.

Table 33 Rockburst hazard based on the SED, B_{i}, and UCS (Lee et al., 2004) .

SED	B_i	UCS (MPa)	Rockburst hazard
<50	<5.75	<78.40	Very low
≈100	≈7.85	≈112.39	Low
≈150	≈9.87	≈138.77	Moderate
≈200	≈12.18	≈161.16	High

Wang et al. (2015) proposed a new method to predict rockburst based on the fuzzy matter-element theory. The matter-element analysis is primarily used to study the problem of incompatibility, and the improved fuzzy matter-element theory evaluation method was employed to assess water quality and showed acceptable results compared with the traditional method. For the proposed rockburst prediction method, the fuzzy matter-element theory was selected, and the rock brittleness coefficient (Eq. (1)), mean stress (Eq. (5)), impact energy tendency, and rock integrity coefficient (Eq. (20)) were introduced as the main influencing factors of rockburst in this model. The Huize Lead-Zinc Mine in China was selected as the study case. This method was applied to different rock strata, and finally, its results were compared with those of the empirical methods of rockburst. Based on the result, the fuzzy matter-element was very efficient for predicting rockburst intensity due to high accuracy, and this model was made based on the empirical method of rockburst. Chen et al. (2003) used the empirical methods of rockburst prediction in conjunction with the artificial neural network for prediction of rockburst. According to the results, this method has an acceptable rockburst prediction accuracy. Dong et al. (2013) performed the Random Forest (RF) method to classify rockburst and its intensity in underground rock project. The main control factors of rockburst, such as the magnitude of in situ stresses, UCS, tensile strength, and elastic energy index (Eq. (13)) of rocks, were selected. Therefore, the RF model and rockburst prediction methods were determined through 36 sets of rockburst predictions. The results showed that the RF model can

accurately classify the rockburst intensity. Feng et al. (2012) studied the rockburst in deep tunnels in Jinping II Hydropower Project. This study aimed to evaluate the rockburst mechanism and its seismicity and intensity before and during the excavation. Thus, laboratory tests and in situ monitoring before and after the excavation process were conducted to analyze the different types of rockburst, such as strain, fault-slip, immediate, and time-delayed rockbursts. The results showed that the evolution of rockbursts consists of generation, opening, closing, and propagation of cracks, in a form of tension, shear, or mixed failure. Rockbursts of different types, that is, strain rockbursts, strain-structure slip rockburst, and exposed different micro-cracking mechanisms in combination of tension, shear, or mixed failure, were considered. The difference with immediate rockbursts is that a quiet period of micro-seismicity before the occurrence of time-delayed rockburst exists. Wojtecki and Konicek (2016) studied the important and effective rockburst factors when the geological conditions of mining are not suitable. Based on the results, the depth of mining, dislocations, and mining remnants are important factors when the mining is located under unsuitable geological conditions. Saeidi et al. (2012) employed empirical methods of rockburst prediction in Sabzkuh Water Conveyance Tunnel as a case study. The Sabzkuh water conveyance tunnel is 11 km in length, passing through high mountains measuring 1200 m. To this end, data have been obtained from laboratory tests, literature reviews, and field studies. The results indicated that the dynamic rockburst should occur in this tunnel. Liu et al. (2013) studied the predictions of rockburst using the Cloud model that represents the overall quantitative features of the qualitative concept. In addition, the attribution weight method was used to quantify the contribution of each rockburst indicator to classification. The results of the computed weight value of the indicator showed that the stress ratio is the most important factor for rockburst occurrence, followed by the elastic strain energy index and brittleness factor. Moreover, the cloud model can predict the rockburst intensity better than the empirical methods of rockburst prediction. Yan et al. (2015) studied the mitigation of rockburst by blasting technique at Jin-ping-I (JPI) and Jin-ping-II (JPII), which are two large hydropower stations. To this end, the elastic strain energy index (Eq. (13)) was used to evaluate rockburst for different excavation footages. Based on the results, the stress-relief blasting method can effectively decrease the stress concentration of the surrounding rocks and reduce the risk of rockbursts. Furthermore, they mentioned that the space between two adjacent relief holes must be less than 2 m in the design of stress-relief blasting to ensure the stress relief effect. In addition, decreasing the excavation footage should be used to control the blasting excavation disturbance in the underground excavation. Guo et al. (2018) studied the effect of saturation time on the coal burst liability indexes. The coal seam water infusion can be used as a suitable technique for rockburst mitigation. To study its effects, they used the strain energy index as one of the empirical methods of rockburst tendency. The results showed that the strain energy index and other factors related to the rockburst tendency decreased as the saturation time increased. Jiang et al. (2010) used the LERR (Eq. (18)) at the Jinping tunnel to determine the conditions causing rockburst. The results showed that the LERR can satisfactorily evaluate the rockburst risk. Afraei et al. (2018) studied those predicting variables with significant effects on the rockburst. They used 188 distinct case histories. For each case history, the predictor variables were overburden thickness, maximum tangential stress in the boundary of opening, UCS of rock, the tensile strength of rock, stress ratio (Eq. (7)), brittleness ratio (Eq. (1)), elastic strain energy index (Eq. (13)), and

one of the four defined classes (none or not-occurred, weak, moderate, and strong) for the qualitative dependent variable of rockburst intensity. The results showed that the predicting variables, such as the maximum tangential stress, stress ratio, elastic strain energy index, tensile strength, and UCS of rock, have significant roles in the rockburst phenomenon. However, the predicting variables, such as overburden thickness, the tensile strength, and brittleness ratio, have no significant effect on the rockburst phenomenon based on case histories. Liu et al., (2015) reported that if the value of UCS is between 100 and 400 MPa, and the rock mass has a high tendency for rockburst. Li and Jimenez (2018) proposed a novel empirical method for a long-term rockburst prediction based on the logistic regression. This model was tested using a database of case histories extracted from the literature and technical report on the underground project. Five possible input parameters, such as tunnel depth, *H*, maximum tangential stress, elastic energy index (Eq. (13)), the UCS of rock (UCS), and the uniaxial tensile strength of rock, were adopted to estimate the probability of rockburst. Last, the results of the new model were compared with those of empirical methods of rockburst. According to the results, the rockburst probability increases with increasing the excavation depth; therefore, elastic energy index and UCS have a similarly significant influence on rockburst occurrence. Li et al. (2017) studied rockburst prediction using incomplete data from Bayesian networks. The five parameters, namely, buried depth in the tunnel, maximum tangential stress (MTS), uniaxial tensile strength, UCS, and elastic energy index, were used to construct the Bayesian network with tree augmented Naïve Bayes classifier structures. Therefore, the novel application of Bayesian network showed acceptable rockburst prediction performance based on the five parameters. Manouchehrian and Cia (2017) investigated the influence of weak planes, such as faults, joints, and dykes, on the occurrence of rockburst in a tunnel subjected to static loads. To this end, they used Abaqus 2D to simulate dynamic rock failure in deep tunnels. The results presented that the rockburst around discontinuities was more violent and the failure zone around the excavation zone was larger. Furthermore, the velocity and the released energy near the discontinuities were higher in comparison with the absence of discontinuities. Therefore, the effect of discontinuities on the rockburst occurrence must be considered in underground excavation. Fakhimi et al. (2016) studied the pillar burst by using the soft loading. To this end, the UCS test was used on sandstone samples to compute the accumulation of the strain energy and find the rupture point of samples. The numerical modeling was also utilized for the rockburst simulation. The effects of different parameters involved in the dynamic rock fracture and strainburst, such as the loading system stiffness, the rock strength, the pillar dimensions, and the rock loading system interface friction coefficient, were considered. According to the results, the pillar diameter and its UCS have an important effect on the induced kinetic energy during a strainburst.

4.5 Discussion

The rockburst prediction approaches can be categorized as empirical, experimental, analytical, intelligent, and numerical methods. Although none of these methods is completely effective or complete, each has its own strengths and limitations. Different assessment indices or indicators are used in empirical methods, having become widely used. It's easy and feasible to employ these methods, which have been shown to be effective in numerous cases. Among stress estimation methods, the rock brittleness coefficient and tangential stress criteria show the most reliable results

in predicting the intensity of rockbursts. They use simple indicators based on a rock mass parameters, which can be evaluated by experimental tests and give realistic values. To predict the intensity of a rockburst, energy methods are more commonly employed than stress methods. Since the results of these methods can be compared to the seismicity data collected from the excavation and the surrounding area, this can provide a clearer insight into the causes of the rockburst. The other reason of using energy methods is that the occurrence of rockburst is closely related to the energy evolution of the rock mass, which includes energy storage, dissipation, and release. Therefore, the criteria based on energy are more likely to reflect rockburst proneness than others. The criteria with multiple indicators, such as the five-actor criterion, have gained favor because it is able to measure rockburst intensity by taking into account more indicators and more significant parameters of the rock. On the other hand, there are some deficiencies with using empirical criteria to predict rockbursts. The majority of empirical criteria are based on a common concept, that is, the ratio of stress to strength, indicating that rockburst is formed by compression. Criteria thresholds are generally determined by the analytical and statistical aspects of the area where rockbursts were observed, or by engineering expertise (Zhou et al., 2012; Feng et al., 2013). In contrast, different scholars use different parameters as evaluation criteria, and the classification of rockburst intensity also differ between them. For example, Kidybinski (1981) proposed that the elastic strain energy index (W_{et}) is recommended to be greater than 5, which indicates a tendency of a strong rockburst. However, on the basis of the experimental results for the Sudbury area (Ontario, Canada) hard rock samples, Singh (1987) proposed that $W_{et} < 10$ is for no or low rockburst intensity. The multiplicity of rockburst criteria made front-line engineers obsessed with discriming the level of the kickoff of a rockburst disaster (Zhou et al., 2018). Moreover, various conditions of geomechanical and geological conditions have been taken into consideration when developing the criteria. Many criteria consider only one component of stress. Strain and stress are second-order tensor variables. Accordingly, estimating rock mass stability based on one extracted component is unreasonable, since the surrounding rock mass is usually under biaxial or triaxial stress conditions, and the strength and deformation properties of rocks are highly affected by multiple stress conditions and the nature of the rock itself. Due to this uncertainty, a universal and practical criterion cannot be identified, and it is necessary to analyze the results of various prediction criteria in depth. Especially, when the empirical criteria are applied, it would be best to specify a range of potential input parameters rather than a single input point, because this would reflect the involved uncertainties. In some empirical rockburst methods like the mean stress index or strength index, the magnitude of principal in situ stress is factored into the equation. The magnitude of in situ stresses in excavation at great depth below surface are estimated rather than the exact value of field stresses. As a result, using these types of empirical methods creates uncertainty, which must be considered during the design and excavation of mines. Also, there are many rockburst reports around the world, however, only a small number of those cases have been described with available or reported data for different representative factors or predictor variables. In each dataset, the values of the following predictor variables are included as: the overburden thickness of the opening in meter, the maximum tangential stress in boundary of opening, the uniaxial compressive strength of rock, the tensile strength of rock, the ratio of the maximum tangential stress to the uniaxial compressive strength of rock (stress ratio), the ratio of the uniaxial compressive to the tensile

strength of rock (brittleness ratio), and the ratio of the elastic energy stored to the dissipated energy (elastic energy index). These documents do not include the detailed descriptions of geological, geomechanical, or technological conditions, any associated seismic events, or any other information factor that affects rockbursts. Furthermore, it is a fact that geological, geomechanical, and technological conditions are difficult to quantify into tangible predictor variables. As for the predictor variables, the maximum tangential stress and stress ratio have been obtained by using different approaches (determination based on in situ measurements or estimating using analytical solutions or numerical models). It is obvious that different methods produce different results. Also, one of the other significant parameters is rock texture, which can strongly influence the petrophysical and mechanical properties of a rock, including its uniaxial compressive strength, elastic properties, and shear strength. Mineral composition, crystal size, rock fabric, alteration degree, grain size and grain shape, weathering, and anisotropy are the most important factors affecting the strength and deformation properties of intact rocks. Also, the discontinuities in the rock, such as macro and micro fractures, bedding planes, schistosity, and faults, make it weaker and control its overall behavior. Accordingly, it appears to be important to understand how rock texture and rock properties interact and subsequently how intensity relates to rockbursts. The rockburst empirical criteria should be developed based on the above factors and validated by a real database. As an outstanding advantages of empirical criteria and in comparison with other rockburst prediction methods like intelligent or numerical methods, they are not highly dependent on the data preprocessing procedure and training parameters. Moreover, stress and energy criteria are widely used in numerical and intelligent methods as the input data. In contrast with numerical methods, which have many limitations in predicting rockbursts behavior, including the complexity of rockbursts, the difficulties in modeling the transition from continuous to discontinuous behavior, and the limitations of the small displacement rule, the empirical criteria are able to predict rockburst intensity in a straightforward way.

5 Summary and Conclusion

Rock mass failure is an important issue in the underground excavation. The risk of rock mass failure increases as the depth of the excavation increases. The presence of an excavation induces an increase of the tangential stress and a decrease of the radial stress, leading to the occurrence of rockburst as an important failure process of brittle and hard rock. The spalling and slabbing forms of rockburst are often observed in underground excavations. Empirical methods have shown acceptable results. However, none of these methods is completely valid, and all of the prediction methods have their own advantages and disadvantages. As mentioned earlier, the predicted rockburst intensity varies considerably from one model to another. The empirical methods are based on one or two stress indices, and the scholar index for all of them is totally different. The energy and stress methods have shown acceptable performance for the evaluation of rockburst tendency. Recent studies developed the rockburst prediction intensity and found the safest rockburst analysis. Typically, one or several rockburst methods are selected, depending on the level of in situ and induced stresses, type of the rock mass, excavation methods, properties of the rock mass, location of tunnel or mine, and dynamic disturbance and experimental instrument. Moreover, the stress and energy methods have been used as a part of the input data in numerical or intelligent

methods. According to the literature review, rock mass brittleness, tangential stress, and Hoek and Brown criteria, as the stress methods of rockburst prediction, are used more among the other stress methods, while the elastic strain energy and linear elastic energy are used as the energy methods of rockburst prediction. However, The ERR cannot determine the intensity, location, and scale of rockburst. Therefore, the new method, FERR, was proposed to help the mining engineering understand the location and scale of rockburst in the underground excavation. However, FERR cannot evaluate the intensity of rockburst. According to the literature, maximum tangential stress, elastic strain energy index, and uniaxial compressive stress and tensile strength are highly efficient in rockburst prediction. Aside from the empirical methods, using numerical modeling is efficient to verify the results of empirical methods with the numerical method. Moreover, the geological structure of mining and the existence of discontinues, such as fault and methods of excavation, have a significant effect on the occurrence of rockburst. For example, delay-rockburst occurs after the excavation because the level of tangential induced stress does not reach to the strength of rock mass. The value of tangential stress reaches the rock mass strength, and rock failure occurs due to the blasting or machine excavation in underground mining or the existence of discontinues. Hence, the external parameters should be considered.

Empirical methods rely on various evaluation indices or indicators, which have become widely accepted. Empirical criteria are easy to employ as they have been shown to be effective in numerous research projects. Simpleness and ease of use are the main advantages of the rockburst empirical criterion and classification method, and mine engineers have used it to identify rockburst events. In the early stages of a project, empirical methods are commonly used to determine the quality of the rock mass and the rockburst of underground openings. Rockburst events are primarily predicted by factors related to stress and energy indexes. These factors are easily determined by the geomechanical laboratory test like uniaxial compressive test, triaxial test and brazillian test. So, these methods could be applied to identify the high risk zone during the excavation. Although predictions of rockburst have received much attention from the research community, many questions remain unanswered. Investigating the following issues may be of interest in the future:

(1) The empirical methods of rockburst are based on the static condition, but there is no method of predicting the effect of dynamic loads on the indicator. Dynamic loads can be formed as extra energy to the excavation area and can increase the energy stored in the rock. It is necessary to develop empirical methods that take dynamic loads into account.

(2) The stress and energy methods of rockburst are based on interpolation of curves and generally have little physical significance, and their validation with real data is limited. By making a large database of rockburst events from all available databases, applying empirical methods to them, and confirming those predictions with real rockburst events, researchers might be able to develop more accurate prediction methods for rockburst.

(3) In the field, rockburst occurrence is strongly related to in situ stress conditions, lithology, excavation depth, rock texture, hydrogeological conditions, and discontinuities surrounding the excavation zone. However, the role of rock texture (Minerals, grainsize, schistosity, etc.) in occurrence of rockbursts remains largely undetermined. So, future studies can focus on the

relationship between rock texture and rockburst intensity, and suggest a number of empirical methods based on the rock texture properties.

Considering these factors, application of these techniques for rockburst prediction will be straightforward and beneficial.

Appendix

List of Symbol			
$2a$	Length of the flaw	S	Turchaninov index
B	Tunnel span or diameter	S_{i}	Stress index
b_{i}	Inclined angle of the flaw	SRF	Stress reduction factor
B_{i}	Rock brittleness coefficient	T	Energetic rockburst indicator
BPI	Burst potential index (%)	T_{s}	Shear strength of rock mass
BIM	Brittleness Index Modified	T_{s}	Tangential stress
c	Cohesion static fraction	T_{d}	Dynamic resistance
D_{t}	Failure duration index	U	Total peak strength of rock mass before rock deformation
C_{g}	Competency factor	U_{t}	Permanent deformation of the rock before the peak
E	Young's modulus (GPa)	$U_{i\,\max}$	Peak value of elastic strain energy before brittle failure
E_{k}	Energy accumulated in the rock mass (KJ m^{-3})	$U_{i\,\min}$	Peak value of elastic strain energy after brittle failure
E_{n}	Energy generated by the tremor in the rock mass	V_{c}'	Initial strain energy of the rock mass
E_{R}	Stain energy retain	V_0^2	Average velocity of broken rock mass ejected to an opening
E_{D}	Permanent strain energy	V_{pr}	Rock elastic wave
E_{i}	Total release energy of failed rock	V_{c}	Strain energy of the rock mass
$E_{\mathrm{k}}^{\mathrm{o}}$	Energy necessary for initiating the rockburst	V_j	Volume of broken element j
E_{t}	Energy of rock fragments after failures	V_{pm}	Rock mass elastic wave speed
ERR	Energy release rate (KJ m^{-3})	V_i	Total volume of broken element in statistic interval i
ESS	ESS	W_{E}	Elastic strain energy accumulated before the rock failure
f_{a}	Factor for scale effect of compressive strength	W_{P}	Plastic strain energy consumed after rock failure
FERR	Fractional energy release rate	W_{et}	Elastic strain energy

H	Overburden depth	σ_c	Uniaxial compressive strength of rock mass (MPa)
K	Rock brittleness index	σ_1	Maximum principal in situ stress (MPa)
K_u	Brittle deformation coefficient	σ_2	Intermediate principal stress (MPa)
K_V	Rock mass integrity coefficient	σ_3	Minimum principal in situ stress (MPa)
L_{ZV}	Break in rock mass volume (t/m^3)	σ_t	Tensile strength of rock mass (MPa)
lg (E/J)	Average logarithm of the radiated energy	σ_v	Overburden stress (MPa)
LESR	Limit energy storage rate	σ_n	Normal stress (MPa)
LERR	Local energy release rate	ε_b	Strain after peak
N	Rock mass number	ε_f	Strain before peak
Q	Barton classification index	μ	Passion ration of rock
R	Elastic strain energy index	γ	Rock density ($kN \cdot m^{-3}$)
LDA	linear discriminant analysis	α	Mean stress (Tao discriminant index)
PLSDA	partial least-squares discriminant analysis	μ_s	Static friction angle
KNN	K-nearest neighbor	η	Burst efficiency ratio
CT	Classification tree	ρ_v	Average density of broken rock
RF	Random forest	QDA	Quadratic discriminant analysis
ABC	Artificial bee colony	NB	Naïve Bayes
SGB	Gradient boosting methods	MLPNN	Multilayer perceptron neural network
RS_i	Strength index	SVM	Support vector machine
RMi	Rock mass index	GBM	Gradient-boosting machine
RBERR	Rockburst energy release rate		
RQD	Rock quality designation		

Acknowledgments

The authors would like to acknowledge the funding received by a grant from Natural Sciences and Engineering Research of Canada (NSERC) for this study.

Declaration of Competing Interest

The authors declare that they have no known competing financial interests or personal relationships that could have appeared to influence the work reported in this paper.

References

Afraei, S., Shahriar, K., & Madani, S. H. (2018). Statistical assessment of rock burst potential and contributions of considered predictor variables in the task. *Tunnelling and Underground*

Space Technology, *72*(11), 250–271.

Ahmed, S. S., ALHeib, M., Gunzburger, Y., & Renaud, V. (2017). Pillar Burst Assessment Based on Large-scale Numerical Modeling. *Procedia Engineering*, *191*, 179–187.

Aubertin, M., Gill, D. E., & Simon, R. (1994). On the Use of the Brittleness Index Modified (BIM) to Estimate the Postpeak Behavior of Rocks. Rock Mechanics Models and Measurements Challenges from Industry. *1st North American Rock Mechanics Symposium*, Austin, Texas.

Avershin, S.G. (1959). Rock Burst, *China Coal Industry Press*, Beijing.

Aydan Ö., & Geniş M., A. T. (2001). Assessment of Susceptibility of Rock Bursting in Tunnelling in Hard Rocks. *Modern Tunnelling Science and Technology*, *67*(1), 369–380.

Bandis, S.C. (1997). Rock characterization for Tunnelling – A Rock Engineer's Perspective, *Feldsbau edition*, 15, 3.

Barton, N., Lien, R., & Lunde, J. (1974). Engineering classification of rock masses for the design of tunnel support. *Rock Mechanics Felsmechanik Mécanique des Roches*, 6 (4), 189–236.

Blake, W., & Hedley, D. G. F. (2003). Rockbursts, Case Studies from North American Hardrock Mines. Book, Chapter 1, 1–15.

Blake., W. (1972). Rock-burst mechanics. *Colorado School Mines*, *67*(1), 1–64.

Board, M. (1996). Numerical examination of mining-induced seismicity. *ISRM International Symposium*, EUROCK 96, Turin, Italy.

Brauner, G. (1994). Rockburst in Coal Mines and Their Prevention. Taylor & Francis Group, 1st Edition, Balkema, Netherlands.

Brady, B. H., & Brown, E. T. (1993). Rock mechanics: for underground mining, *Kluwer Academic Publishers*, Dordrecht, Netherlands.

Broch, E., & Sørheim, S. (1984). Experiences from the planning, construction and supporting of a road tunnel subjected to heavy rockbursting. *Rock Mechanics and Rock Engineering*, *17*(1), 15–35.

Cai, M. (2016). Prediction and prevention of rockburst in metal mines - A case study of Sanshandao gold mine. *Journal of Rock Mechanics and Geotechnical Engineering*, *8*(2), 204–211.

Cao, J.J., Hu, Q.T., & Zhang, Y.J. (2015). Coal rock gas dynamic disaster classification attribute and its prevention practice in deep mine. *Electronic Journal of Geotechnical Engineering*, *20*(19), 11309–11326.

Castro., L.A.M., Bewick, R.P., & Carter, T. (2012). An overview of numerical modellin gapplied to deep mining. Taylor & Francis Group, (Chapter 21).

Chen, B.R., Feng, X.T., Li, Q.P., Luo, R.Z., & Li, S. J. (2013). Rock burst intensity classification based on the radiated energy with damage intensity at Jinping II hydropower station, China. Mechanics and Rock Engineering, *48*(1), 289–303.

Chen, H., Li, N., Nie, D., & Shang, Y. (2003). Prediction of rockburst by artificial neural network.

Yanshilixue Yu Gongcheng Xuebao / Chinese journal of rock mechanics and engineering. 22 (5), 762-768

Colson., C. M. (1950). Rockburst. Master thesis, Missouri S&T University,

Cook, N. G. W. (1963). The basic mechanics of rockbursts. *Journal of the Southern African Institute of Mining and Metallurgy*, *64*(3), 71–81.

Dechelette, O., Josien, J.P., Revalor, R., & Jonis, R. (1984). Seismo-acoustic monitoring in an operational longwall face with a high rate of advance. *South African Institute of Mining and Metallurgy*, 83–87.

Diederichs, M. S. (1999). *Instability of Hard Rock Masses: The Role of Tensile Damage and Relaxation* [Doctoral dissertation, University of Waterloo].

Diederichs, M.S., Carter, T., & Martin, D. (2010). Practical rock spall prediction in tunnels. *ITA World Tunnel Congress*, Vancouver.

Dietz, M., Oremek, G.M., Groneberg, D.A., & Bendels, M. H. K. (2018).What is a rock burst?. *Zentralblatt für Arbeitsmedizin, Arbeitsschutz und Ergonomie*, *68*(1), 45–49.

Dong, L., Li, X., & Peng, K. (2013). Prediction of rockburst classification using Random Forest. *Transactions of Nonferrous Metals Society of China*, *23*(2), 472–477.

Dowding, C. H,., & Andersson, C. A. (1986). Potential for rock bursting and slabbing in deep caverns. *Engineering Geology*, *22*(3), 265–279.

Duan, K., Ji, Y., Wu, W., & Kwok, C. Y. (2019). Unloading-induced failure of brittle rock and implications for excavation-induced strain burst. *Tunnelling and Underground Space Technology*, 84, 495-506.

Du, Z. J., Gao, Y. T., Deng, D. Q., & Han, H. L. (2010). Rockburst Prediction of Deep Mining in Tectonic Stress Mine. *International Mining Forum*. https://file.scirp.org/pdf/29-1.18.pdf

Fairhurst, C. (2003). Stress estimation in rock: a brief history and review. *International journal of rock mechanics and mining sciences*, *40*, 957–973.

Fakhimi, A., Hosseini, O., & Theodore, R. (2016). Physical and numerical study of strain burst of mine pillars. *Computers and Geotechnics*, *74*, 36–44.

Feng, X,. Chen, B., Li, S,. Zhang, C., Xiao, Y., Feng, G,. Zhou, H., Qiu, S., Zhao, Z., Yu, Y., Chen, D., & Ming, H. (2012). Studies on the evolution process of rockbursts in deep tunnels. Journal of *Rock Mechanics and Geotechnical Engineering*, *4*(4), 289–295.

Feng, X.T., Chen, B.R., Zhang, C.Q., Li, S.J., & Wu, S.Y., (2013). Mechanism, Warning and Dynamical Control of Rockburst Evolution Process. *Science Press*, Beijing, pp. 380–391.(in Chinese)

Fisher, J. (2013). Impact of gas emissions on the intiations of coal bumps. *The 23th World Mining Congress*, Montreal, Canada, 396–410.

Gill, D.E., Aubertin, M., & Simon, R. (1988). Une méthodologie d'évaluation du potentiel de coups

de terrain dans les mines d'Abitibi. Colloque sur le Contrôle de Terrain (AMMQ), Val d'Or, Institut de recherche Robert-Sauvé en santé et en sécurité du travail (IRSST).

Gill, D.E., Aubertin, M., & Simon, R. (1993). A practical engineering approach to the evaluation of rockburst potential. *Proceedings of the 3rd International Symposium on Rockbursts and Seismicity in Mines*. Rotterdam, Netherlands. Rotterdam, 63–68.

Gong, F. Q., & Li, X.. (2007). A distance discriminant analysis method for prediction of possibility and classification of rockburst and its application. *Chinese Journal of Rock Mechanics and Engineering*, *26*(5), 1012–1018 (in Chinese).

Goel, R.K. (1994). Correlations for predicting support pressures and closures in tunnels. PhD Thesis, University of Nagpur, India.

Goel, R.K., & Jethwa. J. (1995). An empirical approach for predicting ground condition for tunneling and its practical benefits. 35th US conference on rock mechanics, 431–435.

Grimstad, E. (1999). Experiences from excavation under high rock stress in the 24.5 km long laerdal tunnel. *Proceeding of the International Conference on Rock Engineering Techniques for Site Characterization*, 135–146.

Guo, R., & Yu, R.C. (2002). Design of support work in drift having rockburst danger. *China Mining Magazine, 11* (3), 23–26 (in Chinese).

Guo, W.Y., liang.T.,Yang, Z., & Zhao, T. (2018). Effect of Saturation Time on the Coal Burst Liability Indexes and Its Application for Rock Burst Mitigation. *Geotechnical and Geological Engineering*, *36*(3), 589–597.

Hawkes, I. (1966). Significance of in situ stress levels. In *Proceeding of the first international congress of the international society for rock mechanics*, 1(3).

He, F. (2005). Study on geological hazards in tunneling of deep-buried long tunnels at qinling-dabashan orogen of the three gorges reservoir water diversion project. Ph.D Thesis. China Academy of Geological Sciences, Beijing, China (in Chinese).

He, M., Sousa, L.R., Miranda, T., & Zhu, G. (2015). Rockburst laboratory tests database—application of data mining techniques. *Engineering Geology*, *185*(5), 116–130.

Hedley, D. G. F., (1992). Rockburst Handbook for Ontario Hardrock Mines. *Energy, Mine and Resources,* Ottawa, Canada.

Hoek, E., & Brown, T. (1980). Underground Excavations in Rock, CRC Press, London. 536.

Holland, C.T, & Thomas, E., (1954). Coal mine bumps-some aspects of occurrence, cause, and control. *BuMines, 35*, 65–71.

Hou, F., & Wang, M. (1989). The Rockburst Criterion and Prevention and Cure Step in the Circular Tunnel. The Application of Rock Mechanics in the Project. The Knowledge press, 195–201.

Jiang, Q., Feng, X.T., Xiang, T.B., & Si, G.S. (2010). Rockburst characteristics and numerical simulation based on a new energy index: A case study of a tunnel at 2,500 m depth. *Bulletin*

of Engineering Geology and the Environment. *69*(3), 381–388.

Jiang, Y. D., Pan, Y. S., Jiang, F. X., DOU, L. M., & Ju, Y. (2014). State of the art review on mechanism and prevention of coal bumps in China. *Journal of China Coal Society*, 39 (2), 205-213.

Jiang, Y., Zhao, Y., Wang, H., & Zhu, J. (2017). A review of mechanism and preventation technologies of coal bumps in China. *Journal of rock mechanics and geotechnical engineering*, *9*, 180–194.

Kaiser, P. K., Diederichs, M. S., Martin, C. D., Sharp, J., & Steiner, W. (2000). Underground works in hard rock tunnelling and mining. *ISRM internation Symposium,Melbourne*, Australia, 841–926.

Kaiser, P.K., Tannant, D.D., & McCreath, D. R. (1996). Canadian Rockburst Support Handbook. *Geomechanics Research Center*.

Kaiser, P.K. (2009). Failure mechanisms and rock support aspects. Int. Consultation Report for the Key Technology of Safe and Rapid Construction for Jinping II Hydropower Station High Overburden and Long Tunnels, Jinping II, 62–71.

Kidybiński, A. (1981). Bursting liability indices of coal. *International Journal of Rock Mechanics and Mining Sciences*, *18*(4),295–304.

Lee, S. M., Park, B. S., & Lee, S. W.(2004). Analysis of rockbursts that have occurred in a waterway tunnel in Korea. *International Journal of Rock Mechanics and Mining Sciences*, *41*, 911–916.

Li, N., & Jimenez, R. (2018). A logistic regression classifier for long-term probabilistic prediction of rock burst hazard. *Natural Hazards*, *90*(1), 197–215.

Li, N., Feng, X., & Jimenez, R. (2017). Predicting rock burst hazard with incomplete data using Bayesian networks. *Tunnelling and Underground Space Technology*, *61*, 61–70.

Li, T., Ma, C, Zhu, M. L., & Chen, G. (2017). Geomechanical types and mechanical analyses of rockbursts. *Engineering Geology*, *222*, 72–83.

Li, T., Cai, M.F., & Wang, J.A. (2005). Discussion on relativity between rockburst and gas in deep exploitation. *Journal of China Coal Society*, *30*(5), 562–567 (in Chinese).

Li, T., Cai, M.F., & Cai, M. (2007). Earthquake-induced unusual gas emission in coalmines – A km-scale in situ experimental investigation at Laohutai mine. *International Journal of Coal Geology*, *71*(2–3), 209–224.

Li, Z.H., Wang, E.Y., Ou, J.C., & Liu, Z.T. (2015). Hazard evaluation of coal and gas outbursts in a coal-mine roadway based on logistic regression model, *International Journal of Rock Mechanics and Mining Sciences*, *80*, 185–195.

Lippmann-Pipke, J., Erzinger, J., Zimmer, M., Kujawa, C., Boettcher, M., Heerden, E., Bester, A., Moller, H., Stronik, N., & Reches, Z. (2011). Geogas transport in fractured hard rock - Correlations with mining seismicity at 3.54km depth, TauTona gold mine, South Africa.

Applied Geochemistry, *26*(12), 2134–2146.

Liu, Y., Shu, Y., & Qin, T. (2015). Rock burst forecasting and prevention technology of thin coal seam in xinxing mine. *Electronic Journal of Geotechnical Engineering*. *20*, 4233–4248.

Liu, Z., Shao, J., Xu, W., & Meng, Y. (2013). Prediction of rock burst classification using the technique of cloud models with attribution weight. *Natural Hazards*, 68 (2), 549–568.

Lu, C. P., Liu, Y., Zhang, N., Zhao, T., & Wang, H.,(2018). In- situ and experimental investigation of rockburst precursor and prevention induced by fault slip. *International Journal of Rock Mechanics and Mining Sciences*, *108*, 86–95.

Ma, C. S., Chen, W.Z., Tan, X.J., Tian, H.M., Yang, J.P., & Yu, J.X. (2018). Novel rockburst criterion based on the TBM tunnel construction of the Neelum–Jhelum (NJ) hydroelectric project in Pakistan. *Tunnelling and Underground Space Technology*, *81*, 391–402.

Manouchehrian, M., & Cai, M. (2017). Analysis of rockburst in tunnels subjected to static and dynamic loads. *Journal of Rock Mechanics and Geotechnical*, *9*(6), 1031–1040.

Martin, C. D., & Christiansson, R. (2009). Estimating the potential for spalling around a deep nuclear waste repository in crystalline rock. *International Journal of Rock Mechanics and Mining Sciences*, *46*(2), 219–228.

Meng, F., Zhou, H., Wang, Z., Zhang, L., Kong, L., Li, S., & Zhang, C. (2016). Experimental study on the prediction of rockburst hazards induced by dynamic structural plane shearing in deeply buried hard rock tunnels. *International Journal of Rock Mechanics and Mining Sciences*, *86*, 210–223.

Meng, F., Zhou, H., Wang, Z., Zhang, L., Kong, L., Li, S., Zhang, C., & Hu, S. (2017). Experimental study of factors affecting fault slip rockbursts in deeply buried hard rock tunnels. *Bulletin of Engineering Geology and the Environment*, *76*(3),1167–1182.

Miao, S. J., Cai, M.F., Guo, Q.F., & Huang, Z.J. (2016). Rock burst prediction based on in situ stress and energy accumulation theory. *International Journal of Rock Mechanics and Mining Sciences*, *83*, 86–94.

Misich, I., & Lang, A. (2001). Examples of rockburst damage in Western Australia. *Proceedings of the 5th international Symposium*, South African Institute of Mining & Metallurgy, 59–68.

Neyman, B., Szecowka, Z., & Zuberek, Q. (1972). Effective methods for fighting rockburst in polish collieries. Proceedings of the 5th international strata control conference, 1–9.

Obert., L., & Duvall., W. I. (1967). Rock mechanics and design of structures in rock. Wiley, Newyork.

Ortlepp, W. D., & Stacey, T. R. (1994). Rockburst mechanisms in tunnels and shafts. Tunnelling and *Underground Space Technology*, *9*(1), 59–65.

Palmstrom, A. (1995). RMi-a Rock Mass Characterization System for Rock Engineering Purposes. Ph.D thesis, Oslo University, Norway.

Pan, Y.S. (2016). Integrated study on compound dynamic disaster of coal-gas outburst and rockburst. *Journal of China Coal Society*, 41, (1), 105–112.

Phillips, W. (1944). Rock Bursts and Bumps in Coal Mines. *Transactions of the American Institute of Mining and Engineering*, 104, 55–94.

Pu Y, Apel D B, Lingga B. (2018). Rockburst prediction in kimberlite using decision tree with incomplete data. *Journal of Sustainable Mining*, 17(3), 158–165.

Peng, Z., Wang, Y.H., & Li, T.J. (1996). Griffith theory and rock burst of criterion *Chinese Journal of Rock Mechanics and Engineering*, *15*(1), 491–495 (in Chinese).

Ptáček, J., (2017). Rockburst in Ostrava-Karvina Coalfield. *Procedia Engineering*, *191*,1144–1151.

Qian, Q., & Zhou, X. (2011). Quantitative analysis of rockburst for surrounding rocks and zonal disintegration mechanism in deep tunnels. *Journal of Rock Mechanics and Geotechnical Engineering*, 3 (1), 1–9.

Qiao, C.S., & Tian, Z. Y. (1998). Study of the possibility of rockburst in Dong-gua-shan Copper Mine. *Chinese Journal of Rock Mechanics and Engineering*, *17*, 917–921 (in Chinese).

Rostami, J., Kahraman, S., Naeimipour, A., & Collins, C. (2015). Rock characterization while drilling and application of roof bolter drilling data for evaluation of ground conditions. *Journal of Rock Mechanics and Geotechnical Engineering*, 7(3), 273-281.

Russenes, B. F. (1974). Analysis of rock spalling for tunnels in steep valley sides. Master thesis. Norwegian Institute of Technology, Trondheim.

Ryder J.A. (1987). Excess shear stress in the assessment of geologically hazardous situations. the South African Institute of Mining and Metallurgy, *88*, 27–39.

Saeidi, M., Eftekharib, E., & Taromi, C. (2012). Evaluation of Rock Burst Potential in Sabzkuh Water Conveyance Tunnel, IRAN: a Case Study. 7th Asia Rock Mechanics Symposium, Seoul, South Korea.

Sainoki, A., & Mitri, H. S. (2014). Dynamic behaviour of mining-induced fault slip. *International Journal of Rock Mechanics and Mining Sciences*, 66, 19–29.

Sainoki, A., & Mitri, H. S. (2016). Dynamic Modelling of Fault Slip Induced by Stress Waves due to Stope Production Blasts. *Rock Mechanics and Rock Engineering*, 49(1), 165–181.

Sainoki, A., & Mitri, H. S. (2017). Numerical investigation into pillar failure induced by time-dependent skin degradation. *International Journal of Mining Science and Technology*, 27(4), 591–597.

Sainoki, A., Mitri,H.S., & Chinnasane, D. (2017). Characterization of Aseismic Fault-Slip in a Deep Hard Rock Mine Through Numerical Modelling：Case Study. *Rock Mechanics and Rock Engineering*, *50*(10), 2709–2729.

Sakurai, S. (1993). Back analysis in rock engineering. Comprehensive Rock Engineering -

Excavation, Support and Monitoring. *Pergamon Press*, Oxford, *4*, 543–569.

Shepherd, J, Rixon, L.K., & Griffiths, L. (1981). Outbursts and geological structures in coal mines: a review. *International Journal of Rock Mechanics and Mining Sciences & Geomechanics Abstracts*, *18*(4), 267–283.

Singh, B., & Goel, R. K. (1999). Rock mass classification: A practical approach in civil engineering, Elsevier, Amsterdam

Singh, B., Goel, R.K, Jethwa, J.L., & Dube, A.K. (1997). Support pressure assessment in arched underground openings through poor rock masses. *Engineering Geology*, *48*(1-2), 59–81.

Singh, S. P. (1987). The influence of rock properties on the ocurrence and control of rockburts. *Mining Science and Technology*, *5(1)*, 11–18.

Singh, S. P. (1988). Burst energy release index. *Rock Mechanics and Rock Engineering*, *21*(2), 149–155.

Singh, S. P. (1989). Classification of mine workings according to their rockburst proneness. *Mining Science and Technology*, *8*(3), 253–262.

Spalding, J.(1948). Deep mining, *Mining publication*, London, 14.

Spottiswoode, S. M., & McGarr, A. (1975). Source parameters of tremors in a deep-level gold mine. *Bulletin of the Seismological Society of America*, *65*(1), 93–112.

Sun, X.H., & Li, T. (2011). Prevention Theory and Technology on Compound Dynamic Disaster of Deep Mining in Coal Mine, *Science Press*, Beijing.(in Chinese)

Tajduś, A., Flisiak, J., & Cala, M., (1997). Estimation of rockburst hazard basing on 3D stress field analysis. University of Mining and Metallurgy, Kraków, Poland.

Takla, G., Tacek, J., Holecko, J., & Konicek., P. (2005). Stress state determination and prediction in rock mass with rockburst risk in Ostrava-Karvina coal basin. *ISRM international Symposium*, Brno, Czech Republic.

Tan, Y. A. (1988) Mechanism research and comprehensive evaluation of rockburst. Ph.D Thesis.

Tan, Y. A. (1992). Rockbursting characteristics and structural effects of rock mass. *International Journal of Rock Mechanics and Mining Sciences & Geomechanics Abstracts*, 29(6), 402–403*Sci. Chin*, *35*(8), 981–990.

Tang, B. Y. (2000). Rock burst control using distress blasting. Ph.D. thesis. McGill University, Montreal, Canada.

Tang, L., & Wang, W. (2002). New rock burst proneness index. *Chinese Journal of Rock Mechanics and Engineering* , *21*(6), 874–878 (in Chinese).

Tao, Z. Y. (1988). Support design of tunnels subjected to rockbursting. *Rock Mechanics and Power Plant*, ISRM International Symposium, Madrid, spain.

Terzaghi, K., (1946). Introduction to tunnel geology. *Rock tunneling with steel supports*, 17-99.

Turchaninov, I. A., Markov, G.A., Gzovsky, M.V., Kazikayev, D.M., Frenze, U.K, Batugin, S.A., & Chabdarova, U.I. (1972). State of stress in the upper part of the Earth's crust based on direct measurements in mines and on tectonophysical and seismological studies. *Physics of the Earth and Planetary Interiors*, *6*(4), 229–234.

Vasak, P., Suorineni, F.T., Kaiser, P.K., & Thibodeau, D. (2004). Hazard map approach using space-time clustering analysis of mine-induced microseismicity. CIM conference. Edmonton, Canada.

Wang, Y.H., Li, W.D., Li, Q.G., Xu, Y., & Tan, G. H. (1998). Method of fuzzy comprehensive evaluations for rockburst prediction. *Chinese Journal of Rock Mechanics and Engineering*, *17*(5). 493–501 (in Chinese).

Wang, C., wu, A., Lu, h., Bao, T., & Liu, X. (2015). Predicting rockburst tendency based on fuzzy matter-element model', *International Journal of Rock Mechanics and Mining Sciences*, *75*, 224–232.

Wang, J. A., & Park, H. D. (2001). Comprehensive prediction of rockburst based on analysis of strain energy in rocks. *Tunnelling and Underground Space Technology*, *16*(1), 49–57.

Wang, K., & Du, F. (2019). The classification and mechanisms of coal gas compind dynamic disaster: a preliminary discussion. *Journal of Mining and Mineral Engineering*, *10*(1), 68–84.

Wojtecki, Ł., & Konicek, P. (2016). Estimation of active rockburst prevention effectiveness during longwall mining under disadvantageous geological and mining conditions. Journal of Sustainable Mining, *15*(1), 1–7.

Wu, Y.K., & Zhang, W. B. (1997). Prevention of rockbursts in coal mines in China. *Proceedings of the 4th International Symposium on Rockbursts and Seismicity in Mines*, Rotterdam,361–366.

Xiao Q H，Liu J G, & Lei S X (2016). A new method for calculating energy release rate in tunnel excavation subjected to high in situ stress. *Perspectives in Science*, *7*, 292–298.

Xu C, Liu X L, Wang Z E, Zheng Y L, & Wang S J. (2018). Rockburst prediction and classification based on the ideal-point method of information theory. *Tunnelling and Underground Space Technology*, *81*(1), 382–390.

Xu, J., Jiang, J., Xu, n., Liu, Q., & Gao, Y. (2017). A new energy index for evaluating the tendency of rockburst and its engineering application. *Engineering Geology*, *230*, 46–54.

Xu, M. G., Yao, G., & Yang, Z.O. (2008). Investigation of comprehensive rockburst prediction during deep mining. Boundaries of Rock Mechanics: Recent Advances and Challenges for the 21st Century. 851–856.

Xue Y G, Li Z Q, Li S C, Qiu D H, Tao Y F, Wang L, Yang W M, & Zhang K (2019). Prediction of rock burst in underground caverns based on rough set and extensible comprehensive evaluation. *Bulletin of Engineering Geology and the Environment*, *78*(1), 417–429.

Yan, P., Zhao, Z., Lu, W., Fan, Y., Chen, X., & Shan, Z. (2015). Mitigation of rock burst events by blasting techniques during deep-tunnel excavation. *Engineering Geology*, 188, 126–136.

Yang, J.P., Chen, W.Z., & Zhao W.S.(2017). Geohazards of tunnel excavation in interbedded layers under high in situ stress. *Engineering Geology*, *230*, 11–22.

Yoon, J. S. (1994). Tunnel Engineering, 160–162.

Zanski, J. Podziemna Eksploalogia (1964). *Zloc. Katowice*, 8, English translation.

Zhang, M., Xu, Z.H., Pan, Y.S., & Zhao, Y.S. (1991). A unified instability theory of rock burst and outburst. *Journal of China Coal Society*, *16* (4), 48–53 (in Chinese).

Zhang, G., Chen, J., & Hu, B. (2003). Prediction and control of rockburst during deep excavation of a gold mine in China. *Chinese Journal of Rock Mechanics and Engineering*, *22*(10), 1607–1612 (in Chinese).

Zhang, J.J., & Fu, B. (2008). Rockburst and its criteria and control. *Chinese Journal of Rock Mechanics and Engineering* , *27*(10), 2034–2042 (in Chinese).

Zhang, C. Q, Feng, X. T, Zhou, H., Qiu S L & Wu W P. (2013). Rockmass damage development following two extremely intense rockbursts in deep tunnels at Jinping II hydropower station, southwestern China. *Bulletin of Engineering Geology and the Environment*, *72*(2), 237–247.

Zhao, G., Wang, D., Gao, B., & Wang, S. (2017). Modifying rock burst criteria based on observations in a division tunnel. *Engineering Geology*, *216*, 153–160.

Zhou, X. P., Qian, Q. H., Yang, H. Q. (2011). Rock burst of deep circular tunnels surrounded by weakened rock mass with cracks. *Theoretical and Applied Fracture Mechanics*, *56*(2), 79–88.

Zhou, J., Li, X.B., & Shi, X.Z., (2012). Long-term prediction model of rockburst in underground openings using heuristic algorithms and support vector machines. *Safety Science*, *50*(4), 629–644.

Zhou, K. P., Lin, y., Deng, h. W., Li, J. L, & Liu, C. J.(2016a). Prediction of rock burst classification using cloud model with entropy weight. *Transactions of Nonferrous Metals Society of China* (English Edition), *7*, 1995–2002.

Zhou, J., Shi, X. Z., Huang, R. D., Qiu, X. Y., & Chong, C. H. E. N. (2016b). Feasibility of stochastic gradient boosting approach for predicting rockburst damage in burst-prone mines. *Transactions of Nonferrous Metals Society of China*, *26*(7), 1938–1945.

Zhou, J., Li, X., & Mitri, H. S. (2016c). Classification of rockburst in underground projects: comparison of ten supervised learning methods. *Journal of Computing in Civil Engineering*, *30*(5), 04016003.

Zhou, J., Li, X.B., Mitri, H. S. (2017). A critical survey of empirical methods for evaluating rockburst potential. 15th IACMAG', 19–23 October, China.

Zhou, J., Lia, X., & Mitri, H.S.,(2018). Evaluation method of rockburst: State-of-the-art literature

review. *Tunnelling and Underground Space Technology*, *81*, 632–659.

Zhou, J., Li, E., Wang, M., Chen, X., Shi, X., & Jiang, L. (2019). Feasibility of stochastic gradient boosting approach for evaluating seismic liquefaction potential based on SPT and CPT case histories. *Journal of Performance of Constructed Facilities*, *33*(3), 04019024.

Zhou, J., Guo, H., Koopialipoor, M., Armaghani, D. J., & Tahir, M. M. (2021). Investigating the effective parameters on the risk levels of rockburst phenomena by developing a hybrid heuristic algorithm. *Engineering with Computers*, *37*(3), 1679–1694.

Zhou, J., Koopialipoor, M., Li, E., & Armaghani, D. J. (2020). Prediction of rockburst risk in underground projects developing a neuro-bee intelligent system. *Bulletin of Engineering Geology and the Environment*, *79*(8), 4265–4279.

Zhu, W.C., Li, Z.H., Zhu, L., & Tang, C.A. (2010). Numerical simulation on rockburst of underground opening triggered by dynamic disturbance. *Tunnelling and Underground Space Technology*, *25*(5), 587–599,

Zhu, G.A., Dou, L.M., Cai, W., Li, Z.L., Zhang, M., Kong, Y., & Shen, W. (2016). Case study of passive seismic velocity tomography in rock burst hazard assessment during underground coal entry excavation. *Rock Mechanics and Rock Engineering*, *49*(12), 4945–14955.